A database to compare possible MOFs for volumetric hydrogen storage, taking into account the cost of their building blocks

Jose A. Villajos*, Nikita Gugin, Martin Bienert, Franziska Emmerling, Michael Maiwald

Federal Institute for Materials Research and Testing (BAM), Berlin, Germany.

**Corresponding: jose-antonio.villajos@bam.de*

Abstract

Physical adsorption at cryogenic temperature can increase the density of the stored hydrogen at a lower pressure than conventional compressed gas systems. This mechanism is also reversible and involves faster kinetics than chemical storage. Materials with certain structural and porous properties are necessary for volumetrically efficient hydrogen storage, including large specific surface areas, pore volumes, and appropriated bulk densities. Metal-organic frameworks (MOF) materials are remarkable candidates as adsorbents due to their porous properties and high crystallinity. Large databases like the MOF subset from the CSD or the CoRE-MOF can be used to find the best materials for this application, providing crystallographic information, composition, and porous properties. Herein, we created a database which includes crystallographic and porous properties, metallic and organic composition, and the minimum available cost for their linkers and corresponding suppliers for those for which it was publicly available. The database is also helpful for selecting structures with potential for industrial production and starting material for computational tools like machine learning or artificial intelligence approaches that relate the composition of MOFs with their performance in different applications. A user interface allows for creating customized selections of suitable MOF structures, looking for their porous and crystalline properties, gravimetric and volumetric total uptakes, and metallic and organic composition, as well as properties for the organic linkers like name, molecular mass, price, or presence of specific functional groups. This information was used to select potential structures from up to two metals and two linkers for the volumetric cryostorage of hydrogen.

Introduction

The use of renewable energy is becoming capital to fulfilling the strategic and climate goals worldwide in terms of energy independence and carbon neutrality. However, fossil fuels (gas, coal, and oil) still cover 79 % of the energy production [1], partly due to the difficulty of including the impact of renewables in sectors that are hardly electrified. Examples are the aviation or maritime transport and industrial processes such as the production of ammonia, fertilisers, steel and ceramics [2]. Massive energy storage systems will be even more necessary to balance the intermittent operation of renewable energy sources in power generation in a 100 % green energy scenario. In this sense, hydrogen is a versatile solution that has the potential to partially solve these problems together with other solutions [3-5]. Despite the advantages of hydrogen as an energy carrier, there are limitations to its use, such as the low energy storage density of the gas phase, which requires compression to 30 – 100 MPa [6, 7] or cooling it down for its liquefaction at –253 °C [7, 8].

During physisorption, hydrogen molecules cover solid surfaces due to van der Waals, electrostatic, or orbital interactions [13, 14], without rearrangement of atoms or formation of new chemical bonds [9], which allows fast and reversible operation compared to chemical storage methods such as metal hydrides or liquid carriers [10-12]. The interaction energy between the hydrogen molecules and the adsorbents is so low that cryogenic temperatures of ca. –196 °C are required to achieve a significant increase in volume compared to the compressed gas at the same pressure and temperature [13, 14]. However, liquid nitrogen is also used during the hydrogen liquefaction process, which is considered a viable option for large-scale storage or transportation [8, 15]. Cryoadsorption further improves the cryocompression technique, reaching higher storage density for the same pressure and temperature [16, 17]. Finally, physisorption-based storage systems can be an alternative to mechanical compressors because, as thermally driven compressors, they have a smaller size due to the adsorption-desorption cycle, low maintenance costs due to the absence of moving parts, no noise and vibration, and a potentially favourable energy balance [16, 17].

In recent decades, different porous materials like zeolites and carbons have been investigated for hydrogen cryoadsorption [12, 14, 18]. Ultraporous materials like COFs (covalent organic frameworks) and MOFs (metal-organic frameworks) provide a higher storage uptake because of their large surface areas, high void fractions, and reduced densities. COFs are even less dense materials, which is beneficial for the gravimetric storage capacity, but many of these structures collapse after removing the solvent molecules [19, 20]. The MOFs used for hydrogen adsorption are crystalline coordination polymers with three-dimensional porosity where metal atoms or clusters are linked to organic molecules by electron-donor groups [21-23]. The different nature of metals and organic linkers and their possible geometries and topologies are the reasons for the more than 70,000 MOF structures that have been experimentally synthesised so far [24].

Hydrogen adsorption in MOFs has been intensively investigated since 2003 as a consequence of the initially promising hydrogen uptake of the carboxylate-like material MOF-5 [25], a crystalline Zn-terephthalate with a hydrogen uptake of 7.1 wt. % at –196 °C and 40 bar [26]. The promising hydrogen storage capacity of MOF-5 was lately surpassed by materials such as NU-100 and MOF-210, which are currently among the best-performing MOFs for gravimetric hydrogen storage at –196 °C with 14.1 wt. % at 70 bar [27, 28] and 15 wt. % at 80 bar [29]. However, a high gravimetric hydrogen uptake in ultra porous materials is not necessarily related to a high volumetric storage density due to the low density of some structures, and, for those, the volumetric gain achieved by adsorption can drop to negative values at high-pressure compared to simply compressed gas [30-32]. That is the case for ultra porous materials NU-100, -108, -109, -110, MOF-180, -200, -210, and -399 [33-35]. An adequate balance of the specific surface area and density is necessary for materials to show simultaneously high gravimetric and volumetric storage densities [35]. Table 1 shows examples of MOF materials that would meet both gravimetric and volumetric DOE's targets for hydrogen storage in 2025, operating at –196 °C. However, the reported volumetric uptake quantities are not readily comparable because different definitions of density and different approaches to measuring sample volume are used. In some cases, the volumetric storage density is obtained by multiplying the measured or calculated gravimetric uptake times the crystal density, obtaining the maximum possible storage density assuming perfect single crystals.

For some applications, the crystalline and porous properties of the solids are directly related to their performance. That is the case for hydrogen storage at cryogenic temperatures. Besides, MOFs have theoretically and experimentally outperformed some state-of-the-art materials for many applications, but their still-high commercialization cost hampers their large-scale usage [36-41]. In addition to the

solvents, catalysts, structuring agents and conditions used for synthesis, purification, and activation [37, 42-44], the organic and metallic starting materials influence the final cost and industrial feasibility of these compounds. Reagent availability, cost, ease of procurement, handling and even strategic or environmental constraints vary for different metallic and organic starting materials. Some organic linkers are not commercially available and require complicated multi-step chemical synthesis pathways. Crystallographic and porous properties are available in different databases containing several thousand structures, like the MOF-Subset from the CSD (Cambridge Structural Database) [24] or the CoRE MOF database (Computationally Ready Experimental MOFs) [45]. However, to the best of our knowledge, there is no database of MOFs collecting normalised names or identifiers of the linkers, differentiating among different ones, their commercial availability and, for those available, their price.

Table 1. Gravimetric and volumetric uptakes of MOF materials that fulfill the gravimetric and volumetric DOE targets for 2025 at -196 °C (5.5 wt. % and 40 g/L) [46-48].

MOF	BET[a] (m^2/g)	V_p (cm^3/g)	Gravimetric uptake[b] (%)	Volumetric uptake[c] (g/L)	Pressure[d] (bar)	Reference
MOF-5/ IRMOF-1	3,800	>1.18[f]	7.1 (10.0)	(66)	40 (100)	[26]
MOF-177	4,750	1.69	6.9 (10.2)	(48)	72	[49]
MOF-205	4,460	2.16	7.0 (12.0)	(46)	80	[50]
MOF-210	6,240	3.60	7.9 (15.0)	(44)	(80)	[51]
IRMOF-20	3,409[g]	1.53[g]	6.7 (10.0[e])	(61[e])	80	[52]
Mn-BTT	2,100	0.79	5.1 (6.9)	(60)	90	[53]
SNU-77H	3,670	1.52	8.1 (10.9)	(64)	90	[54]
SNU-5	(2,850)	1.00	5.2 (6.8)	(52)	50	[55]
UMCM-150	2,300	1.00	5.7 (7.0[e])	(48[e])	45	[56]
NOTT-101	2,316	0.89	5.5[h] (6.2)	(43)	25 (60)	[57]
NOTT-102	2,942	1.14	5.7[h] (6.7)	(42)	30 (60)	[57]
NOTT-103	2,929	1.14	6.0[h] (7.2)	(50)	28 (60)	[57]
NOTT-110	2,960	1.22	5.4[h] (7.6)	(47)	(55)	[58]
NOTT-111	2,930	1.19	5.4[h] (7.4)	(45)	(48)	[58]
NOTT-112	3,800	1.62	7.1[h] (10.0)	(50)	35	[59]
NOTT-113	2,970	1.25	5.1[h] (6.7)	(42)	30 (60)	[59]
NOTT-114	3,424	1.36	5.0[h] (6.8)	(42)	30 (60)	[60]
NOTT-115	3,394	1.38	5.6 (7.5)	(49)	33 (60)	[60]
NU-100/ SNU-610	6,143	2.82	9.04 (14)	(47)	70 (100)	[27, 28]
PCN-11	1,931	0.91	5.0 (6.0)	(45)	45	[61]
PCN-46	2,500	1.01	5.3 (6.9)	(46)	32 (97)	[62]
PCN-61	3,000	1.36	5.9 (7.2[e])	(43[e])	35	[63]
JUC-62	n.a.	0.88	(4.7)	(53)	40	[64]

a: in parenthesis: *Langmuir area*. b & c: excess (total) uptakes. d: saturation pressure (in parenthesis if pressures for total and excess are different). e: calculated. f: [46]. g: [65]. h: collected data by gravimetric devices, corrected with the buoyancy of solid and adsorbed phase (ρ = 0.0708 g/cm³).

The actual chemical composition of MOF materials is available in the CSD, or it can be extracted using a provided algorithm by the CCDC (Cambridge Crystallographic Data Center), isolating the name of metallic and organic components of MOF frameworks [66]. The obtained information is not unified because of the large number of structures and the use of diverse nomenclature rules to name the organic components. A recently reported algorithm [67] deconstructs the crystallographic information

into chemical identifiers for MOF's metallic and organic building blocks, identifying the organic molecules by using canonical SMILES strings (Simplified Molecular Input Line Entry System) [68, 69] or InChIKey codes (International Chemical Identifier) [70]. Different Machine-Learning (ML) approaches have been reported starting from this strategy to find the relationship between structural and chemical properties of MOF materials with their performance in different applications, like volumetric hydrogen deliverable capacity and selectivity in ethylene/ethane separation [71-74]. Also, recent ML approaches predict porosity [75] and their synthetic conditions [76] from the metallic and organic composition of MOFs.

In this work, we combine both approaches to obtain the organic composition of MOFs and produce a list of structures showing the organic and metallic composition of potentially useful MOFs for volumetric hydrogen storage at –196 °C and 100 bar. The potential industrial feasibility was compared considering the nature and current cost of linkers for laboratory use. Starting from a selection of 8,768 structures from the 2019 CoRE MOF database, in which a significant proportion of materials have never been tested for hydrogen adsorption, we developed a database of approximately 4,000 MOF structures with an estimated hydrogen storage density higher than 40 g/L, synthesised from abundant and industrially relevant metals. While this database was developed with hydrogen adsorption properties in mind, it could also be applied for selecting potential materials for other applications where porosity is the critical property and can even be used as starting information for ML approaches to relate MOF composition to other targeted properties or their application.

Methods and data

The CoRE MOF (Computational-Ready Experimental MOFs) database contains 8,768 optimised MOF structures in which solvent molecules, coordinated or not, have been removed from the cavities. This database provides structures' identifiers used in the MOF-subset of the Cambridge Structural Database (CSD), their porous properties like gravimetric and volumetric accessible areas, pore volume, void fraction, and density; and the metallic composition as well as the potential presence of open metallic sites (OMS) [45]. The gravimetric hydrogen uptake was calculated for these structures using an estimation method starting from the porous properties of structures with a higher pore volume than 0.3 cm^3/g [77]. The volumetric uptake of each structure was calculated by multiplying the gravimetric uptake by the corresponding crystallographic density.

The organic composition of MOFs is not defined in the CoRE MOF database nor the CSD MOF subset, but can be determined from the crystallographic information in the CSD and has been coded as MOFid codes for most of these structures [67]. MOFid consists of Canonical SMILES strings coding the inorganic and organic chemical components, topology, and identifier of the corresponding MOF structure. Some of the SMILES strings provided correspond to fragments or substructures of linkers and could indicate more components than those actually present in the material, as these fragments are identified as different substances. This algorithm also provides a second code, the MOFKey, linking the metallic elements and the InChiKey (a fix-length format of the International Chemical Identifier) of the linkers present in the structure. However, the same limitations affect MOFKey and MOFid since they both start from the deconstruction of the crystallographic data. Therefore, the MOFid and the MOFKey do not code the organic composition of ca. 10 % of the structures in the CoRE MOF database.

In this work, the chemical composition of a selection of 3,786 structures with higher volumetric hydrogen uptake than 40 g/L made out of industrially important metals (Al, Ca, Cd, Cr, Cu, Fe, Li, Mg, Mn, Mo, Na, Ni, Sn, Sr, Ti, V, Zn, and Zr) was directly obtained from the CSD. The software ConQuest (under license of CCDC) generates a ".cfg" file compiling the deposited crystallographic information and chemical composition for each structure. This composition was split into its components (linkers, solvents, other coordinated molecules, and extra-framework substances) by performing a described algorithm in ESI in MS Excel. Common solvents such as dimethylformamide, ethanol, methanol, and water were removed from the composition of the materials, leaving other organic molecules such as structuring agents (SDA) or charge-balancing ions. In total, 2,207 organic molecules appear in this selection, some of which are named following different nomenclature rules (i.e., terephthalate, 1,4-benzenedicarboxilate, or benzene-1,4-dicarboxylate).

To normalize the nomenclature and provide a unique identifier for all the organics, 1,868 of the provided names were converted into their corresponding SMILES strings by using the code OPSIN from the University of Cambridge [78] and then converted into canonical SMILES strings with the free software Open Babel [69]. The MOFid and MOFKey codes from ref. [67] were used to identify the organic molecules without SMILES strings. The public database PubChem [79] was used to get information for each SMILES string, like molar mass, CAS number, and IUPAC's name for the parental compounds. Before searching this information for a substance, the SMILES string of deprotonated molecules, as they appear in the MOF composition, were protonated. As an example, the deprotonated carboxylate moiety is represented as "C(=O)[O-]", whereas "C(=O)O" indicates the protonated form. The identified organic molecules in the database were unified in 725 compounds and classified as linkers or non-linkers. Prices and purities were found in available links to vendors' websites in ChemSpider, starting from CAS numbers or SMILES strings for each substance. For each vendor, the price for the largest packing was collected, and the lowest price-per-gram was selected for each substance. The price for 499 organic substances was found, updated in February 2022.

A Python-based user interface facilitates the search of structures within this database, using properties of the structures (crystallographic and porous properties, density, gravimetric or volumetric hydrogen uptake at 77 K and 100 bar, the presence of Open Metal Sites, the nature of the metallic or organic components, and the price-per-gram of the used organics), the information of the organic molecules (name, CAS number, molar mass, price-per-gram, functional group), even giving the possibility to filter structures by their used linkers. In addition, it is possible to specify the number of organic or metallic components (as one, two, three, or any) and consider including structures with non-linker organic molecules. Finally, the interface exports data into .csv files for structures and their used linkers. Figure 1 shows an example of a search of MOF structures consisting of one metal combined with up to two organic molecules, only containing linkers cheaper than 26 €/g while not allowing non-linker organic molecules. The interface shows 315 results in the selected MOFs window, detailing for each structure the CSD reference, the structure's name, its porous and crystalline properties, gravimetric and volumetric total uptakes, and the metallic and organic composition. With the same limitations regarding the cost applied to the organic search parameters, it also displays a list of 261 linkers cheaper than 26 €/g, for which the normalized name, CAS, alternative names, SMILES strings, and molecular weight are displayed. To access more detailed information, like prices and purities from different vendors of the linkers in the database, one may double-click an entry in the table to open a window (see Figure 2). An online version of this tool is available at https://mofdb-bam.de with a centralized database, providing the same functionality as the previously described user interface. Up to now, the price of the linkers needs manual updating.

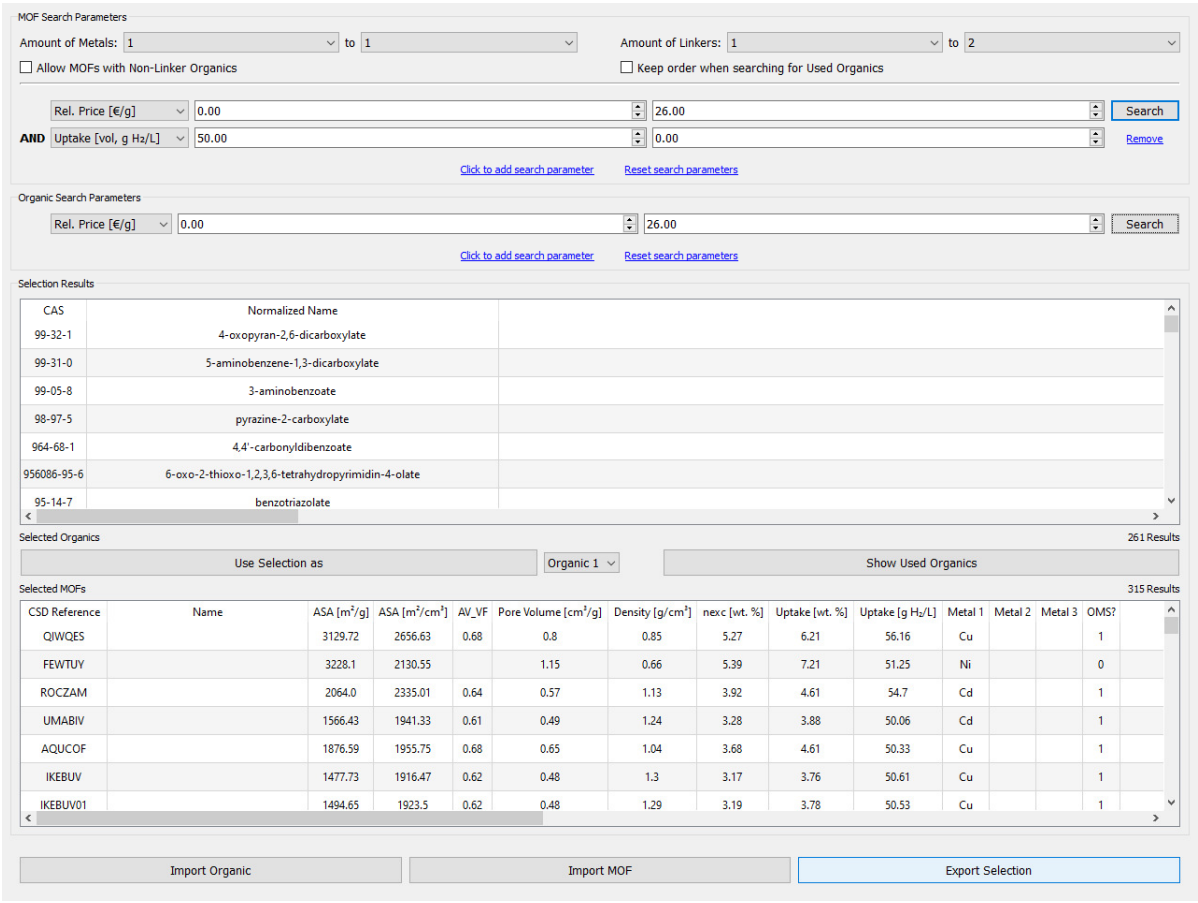

Figure 1. User interface for searching MOF structures in the database for cheap MOFs.

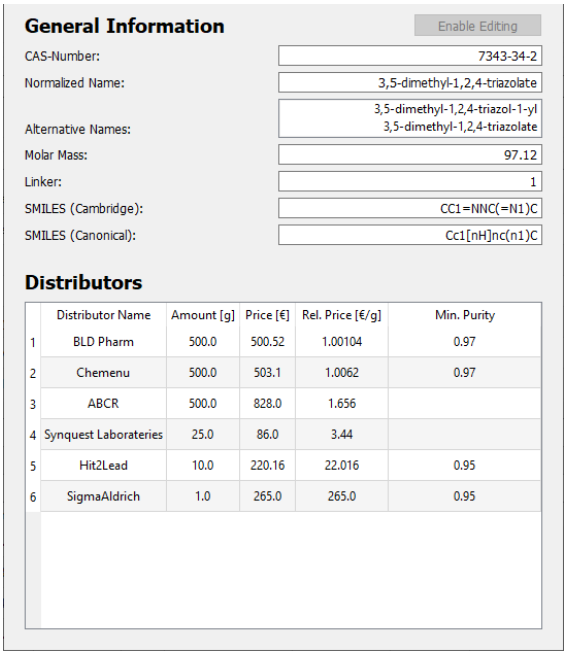

Figure 2. Information of organic molecules in the database, provided via the user interface.

Potentially affordable MOFs for cryogenic hydrogen storage

From the 9,146 structures in the CoRE MOF ASR (all solvent removed) database [45], 8,626 are contained in the CSD, and it is possible to obtain their composition. From this list, 6,913 structures have a higher calculated pore volume than 0.3 cm^3/g, the lower limit set in the H_2 uptake estimation procedure [80]. Among these, 5,295 materials would ideally meet the target of 40 g/L for 2025. Some hydrogen uptakes could be overestimated due to the reported geometric areas, sometimes higher than the experimentally measured values, because of the used estimation procedures or the measuring approaches themselves, presence of structural defects in the experimentally-obtained structures, differences in their activation, frameworks' flexibility, polymorphism, and instability of crystalline phases to preparation/operation conditions during porosity measurements [81-84]. Also, the structural simulations and optimisations before calculating the porous properties of this selection of MOFs do not consider the possible structural changes in the crystals after removing solvent molecules, such as after creating exposed-metal sites or removing structure-directing agents (SDA) or charge-compensating substances [45]. An example is the material Zn-PyDC (CSD code BUKMUQ), made out of pyridine-3,5-dicarboxylic acid and Zn, whose measured surface area (A_{BET} = 546 m^2/g) is significantly lower than the calculated one (3,160 m^2/g) due to its guest-dependent flexible structure [85]. According to the database, the mixed-linker material Zn_4-Ser_2-BDC from terephthalic acid and D-serine (CSD code RAPYUE) is a high-density hydrogen absorber, but its measured porous properties are much lower than the calculated values. However, an uptake of 1.8 wt. % H_2 was experimentally measured at –196 °C and 30 bar, surpassing the estimated uptake from Chahine's rule [34]. Calculated SSA values for materials Me_2-$DOBQ_3$ (Me=Ni, CSD code OWITOE, Fe, OWITUK, Zn, OWIVAS, Co, OWITEU, and Mn, OWITIY; DOBQ: 2,5-dioxy-1,4-benzoquinone) are between 4,800 – 5,100 m^2/g with a 77 % of void volume. However, the tetrabutylammonium countercations were computationally removed from the cavities before the porosity calculations, which may not be possible to perform experimentally.

The Core MOF database includes the metallic information for each structure, making it possible to screen among structures made out of feasible metals. The most affordable metals are abundant in the Earth's crust, non-noble, and industrially relevant [86]. Cheaper metals with higher abundance than W are selected (Al, Ca, Cd, Cr, Cu, Fe, Li, Mg, Mn, Mo, Na, Ni, Si, Sn, Sr, Ti, V, Zn, and Zr), thus reducing the list to 3,536 materials. Zn is the most frequent metal in the database and the cheapest one, with 1,195 derived deposited structures (1,132 with Zn as individual metal), 744 of which potentially exhibit open metallic sites (OMS), preferential adsorption sites for gases like hydrogen [87]. The second most-used metal is Cu, with 940 structures (872 as single metal), a noble metal considered herein due to its industrial importance and potential for synthesising MOF for hydrogen storage. From this selection, 845 materials show OMS. Therefore, the storage density could be even higher than the estimated value. MOFs made out of toxic metals like Be or Hg are not considered, except the 453 MOFs from Cd, a toxic metal five times cheaper than Cu. Cd can be obtained from Ni-MH batteries wastewater and from recycling solar cells, and these MOFs are an opportunity for removing and recycling this metal's waste. Other attractive metals are Fe, a cheap metal that can be reused from recycling scraps, Mg, Mn, Cr, and Zr. This last is present in some materials with the highest structural stability among MOFs, like UIO-66 [88].

The costs for 499 of the identified linkers with their CAS number were found on the websites of the chemical suppliers. Figure 3 compares the corresponding minimum hydrogen storage density for MOFs made out of these linkers, considering structures with only one linker and one metal without non-

linker organic molecules (e.g., naphthene, ammonium derivatives, monocarboxylic acids like benzoic acid, phenol,…), that can act as SDAs, charge-compensating ions, or capping agents. The volumetric uptake corresponds to the centre of each circle, and its diameter is proportional to the number of deposited structures for each linker. According to this comparison, higher minimum volumetric storage density values are generally reached in constructed MOFs from more expensive linkers. This is partly because cheaper linkers are increasingly used in synthesising MOFs, which more often results in materials with a low surface area. More expensive linkers often aim to synthesise specific MOFs with enlarged surfaces by following the principles of reticular chemistry [36]. However, the volumetric area of MOFs, which is related to volumetric uptake, depends not only on the specific surface area but also on the material density. Therefore, it is also possible to achieve a volumetric storage density with relatively cheap linkers, such as terephthalic acid (0.0215 €/g) or trimesic acid (0.0989 €/g).

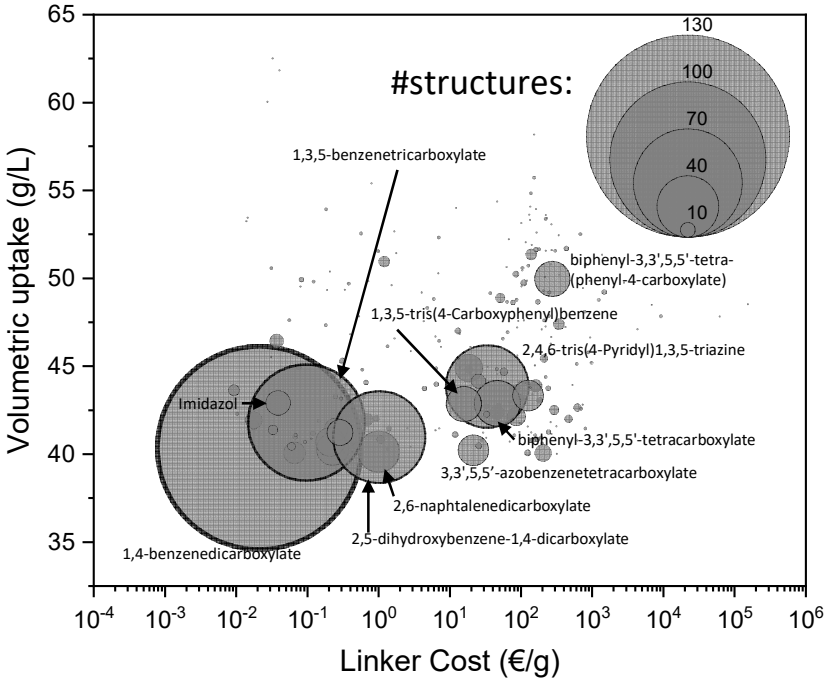

Figure 3. Minimum H_2 storage density achieved for MOFs as a function of the cost of their linkers.

The found cost of linkers varies in a 10^7 order of magnitude, from 0.01 €/g for fumaric acid to 162,540 €/g for 2-pyridin-4-yl-1H-imidazole-4,5-dicarboxylic acid. Examples of cheap linkers for current production of commercially available MOFs are 1,4-benzenedicarboxylic or terephthalic acid in MOF-5, 2-aminobenzene-1,4-dicarboxylic acid in MIL-53, 1,3,5-benzenetricarboxylic acid in HKUST-1, fumaric acid in Mg-Formate, and 2-methylimidazol in ZIF-8. More expensive substances like 1,3,5-tris(4-Carboxyphenyl)benzene and 3,3',5,5'-Azobenzene-tracarboxylic acid can be found in commercially available materials MOF-177 and PCN-250(Fe), respectively. In our selections, we assumed the upper-cost limit for likers' cost as the most expensive substance used in these commercially available MOFs. However, further optimisation of the linkers' production is necessary for industrial production. For instance, for using MOFs in methane storage, cheaper linkers than 10 $/kg are necessary to limit the MOF cost below 70 $/kg [42, 43].

Table 2 shows the compositions of 666 MOFs from individual metals, considering cheaper linkers than 3,3',5,5'-Azobenzenetetracarboxylic acid (included), with a higher minimum estimated hydrogen storage density than 40 g/L. The most common metal-linker combination is 1,4-benzenedicarboxylate (H_2BDC, CAS No. 100-21-0, 0.02 €/g) with Zn, yielding 32 different entries in the database and

constituting one of the cheapest combinations of metal-linkers to synthesize MOFs including the archetypal MOF-5 (MIQBAR), the porous material with the highest measured volumetric hydrogen uptake by cryoadsorption (see Table 1). The material Zn_3-BDC_4 (CSD reference UFENAW, see Figure 4) is an interpenetrated network with 4,090 m^2/g of SSA and 0.98 cm^3/g of pore volume and would store the highest amount of hydrogen per volume (62 g/L) among terephthalate based MOFs. Table S1 in ESI shows all structures from this linker after duplicates' removal (remaining the representative material with the smallest volumetric area).

Table 2. Number of Linker-metal combinations for MOFs with estimated volumetric uptake higher than 40 g/L. Only linkers with available prices are considered in the table.

Linker CAS	Al	Ca	Cd	Cr	Cu	Fe	Li	Mg	Mn	Na	Ni	Sr	Ti	V	Zn	Zr	Total	Price (€/g)
100-21-0	9	3	5	10	1	5		2	18		1	5		19	32	15	125	**0.0215**
554-95-0			11	2	25	4	1	3	2		3				24		75	**0.0989**
610-92-4		2	1		7	19		9	6		6	1			9		60	**1.0509**
1141-38-4	1					1		5	6						14		27	**1.0354**
50446-44-1		1	2		13				1		1				5		23	**16.3744**
4282-31-9		4			2			3	2			4			1	5	21	**0.2313**
365549-33-3	1		3		3	2		2	2		2				5		20	**22.2912**
553-26-4		1			13	1					2				2		19	**0.2150**
14389-12-9			7		11												18	**19.2640**
787-70-2			1	2		2		2	4					1	4	1	17	**0.2941**
693-98-1			3												13		16	**0.0396**
499-81-0		1			7			4	1						2		15	**0.2571**
1453-82-3			7		2				2	1	2						14	**0.0671**
288-32-4			1												10		11	**0.0181**
288-88-0			1		5						1				2		9	**0.0378**
10312-55-7	3							2					1		2		8	**0.7100**
110-17-8	1					3									2	1	7	**0.0095**
37718-11-9					2										5		7	**1.2384**
89-05-4			1												5		6	**0.0335**
121-91-5	1								1		1				3		6	**0.0180**
2215-89-6					4			1							1		6	**0.1204**
100-26-5		1													4		5	**0.5117**
118996-38-6	2				1										2		5	**19.0920**
499-80-9		1						4									5	**1.0991**

In addition to the costs of a compound, its operation stability is capital for the final application. This is indeed the weakest point of the material MOF-5, whose high performance in hydrogen storage and low cost are compensated by its low stability to the action of atmospheric humidity. Although the stability to environmental conditions and operation must be tested individually for each MOF, we can relate the composition and stability of the MOF to water and acidic/basic media generally [89]. Mainly, carboxylates act as hard Lewis bases, involving a stronger metal-organic bond when coordinating hard Lewis acids, like high-valence metal cations (usually, Me^{3-4+} like Al^{3+}, Cr^{3+}, Fe^{3+}, Ti^{4+} or Zr^{4+}). In this sense, combinations of terephthalic acid with V, Mn, and Zr, with higher oxidation numbers than Zn^{2+}, might yield more robust structures in contact with ambient moisture during handling or water as a pollutant in hydrogen from electrolysis. Other potentially stable structures with remarkable storage capacities are MIL-88B (KUXREC), showing OMS of Fe, and UIO-66 (RUBTAK03), a known Zr-MOF for its exceptional mechanical and hydrothermal stability [90]. Besides, materials MIL-53, -101, and -47 are made out of metals Cr, Al, and V and could store between 42 – 45 g/L of hydrogen.

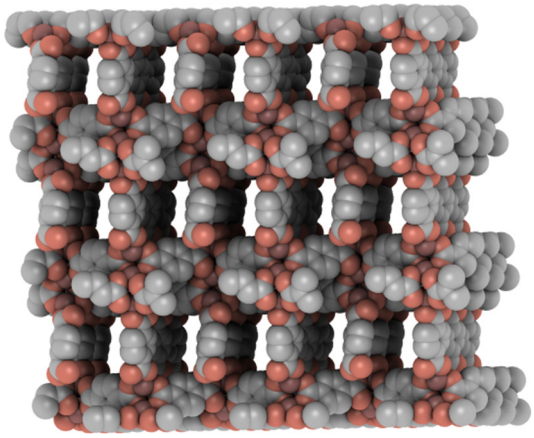

Figure 4. Zn_3-BDC_4 (CSD code UFENAW). Created with visualising software iRASPA [91].

The next most common linker is 1,3,5-benzenetricarboxylic acid (H_3BTC, CAS No. 554-95-0, €0.10/g) or trimester acid, for which Cu is the most common metal with 25 structures, many of which correspond to the material HKUST-1 or Cu-BTC (CSD code DIHVIB, see Table S2 in ESI), one of the first MOFs tested in hydrogen adsorption [65]. Structures Zn_2-BTC (RIZXUT) and Cd_2-BTC (QISNAJ) show the highest estimated volumetric uptake in this list. Structure BIT-103 (CSD code VEHJOJ, see Figure 5) could potentially store 54 g/L within its tridimensionally connected porosity, as well as structure FJI-3 (FIWKUT). All these structures with potential OMS are promising materials for volumetric hydrogen storage if their structures are stable after removing coordinated solvent molecules to the metallic positions. The structure Fe_6-BTC_3 (CSD code NINVAI), similar to HKUST-1 but with Fe instead of Cu, also exhibits OMS and could show higher stability, as well as structures Mn_2-BTC (FUTCAZ), Mn_3-BTC_2 (DEPXOM), and Cr_3-BTC_2 (ZIGFIG), with higher storage density than 50 g/L.

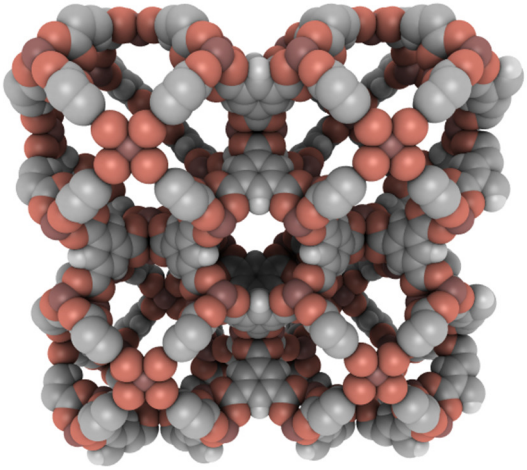

Figure 5. Material BIT-103 or Zn_{11}-BTC_6 (CSD code VEHJOJ). Created with iRASPA [91].

The third most frequent linker is 2,5-Dihydroxybenzene-1,4-dicarboxylic acid (H_2DOTP, CAS No. 610-92-4, 1.05 €/g, Table S3 in ESI), used to synthesise the materials M-MOF-74/M-CPO-27/M-DOTP, where metals connected by oxygen atoms from the linker form rod-like metallic clusters and one-dimensional hexagonal channels [65]. These OMS-rich materials involve a high interaction with hydrogen molecules, reaching 13.5 – 14 kJ/mol for material Ni-CPO-27 [92, 93], the highest measured enthalpy of adsorption among physisorbents. Materials with Zn, Ni, Fe, Mn, and Mg are included in this database, for which the highest uptake is 47 g/L for the material out of Zn (see Figure 6). However, the volumetric uptake of these materials could be underestimated in this work because the estimation

procedure does not consider the higher superficial packing density of the sorbed hydrogen over surfaces with a high concentration of OMS [92-95]. Also, these materials show reduced stability to moisture when heated above 150 °C due to water's catalytic decomposition on their OMS [96]. From this selection, material Sr-DOTP (CSD code YUFLOC) has the highest calculated volumetric uptake. This structure also exhibits a different crystal phase than materials M-DOTP because oxygens in positions 3 and 5 of the linker are not coordinated to metals and do not form rod-like metallic clusters.

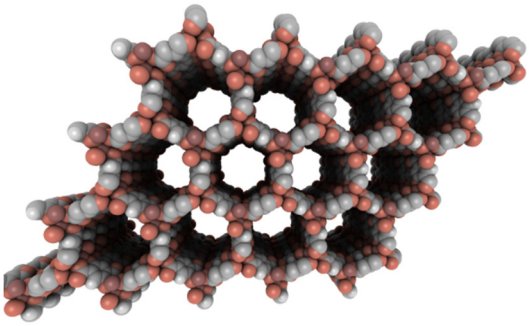

Figure 6. Material Zn-MOF-74 or Zn-DOTP (CSD code WIZDEP). Created with iRASPA [91].

Several remarkable structures have a potential storage capacity higher than 50 g/L when using 2,6-Naphthalenedicarboxylic acid (H_2NDC, CAS No. 1141-38-4, 1.03 €/g) to coordinate Zn nodes (see Table S4 in ESI). Examples are isostructural structures to material MOF-5 like Zn_4-NDC_3 (EDUTUS), with a similar volumetric uptake, or the interpenetrated IRMOF-8 material (Zn_4-NDC_3, WORLAS). Material UTSA-38 (CAGSAG, see Figure 7) and CAU-3-NDC (Al_2-NDC, with CSD code CAXSUR) have not-interpenetrated structures with 3D connected pores and the potential for storing almost 50 g/L. In principle, higher stability to moisture is expected for these structures because of the hydrophobicity of the NDC linker and the presence of Al^{3+} cations.

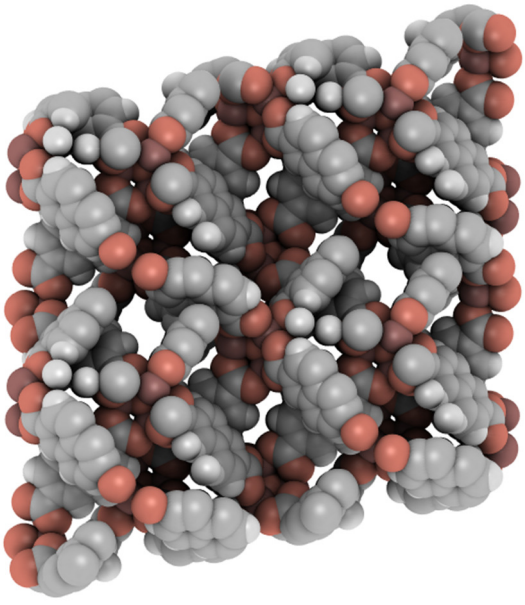

Figure 7. Material UTSA-38 or Zn_4-NDC_3 (CSD code CAGSAG). Created with iRASPA [91].

All MOFs out of 1,3,5-tris(4-Carboxyphenyl)benzene (H_3BTB, CAS No. 50446-44-1, 16.37 €/g, see Table S10 in ESI), the linker of the material MOF-177, contain divalent metals. Structure MOF-14 (QOWQUO, see Figure 8) with Cu could potentially store 50 g/L of hydrogen and has been synthesized by a solvent-free ball-milling approach [97], which can be beneficial in reducing its production cost.

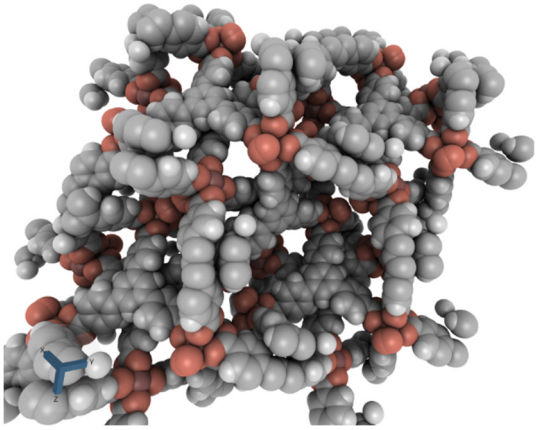

Figure 8. Material MOF-14 or Cu_3-BTB_2 (CSD code QOWQUO). Created with iRASPA [91].

The Cu-based MOF-107 (AGAXOV) shows the highest volumetric storage density among the 21 derivatives from Thiophene-2,5-dicarboxylic acid (H_2TDC, CAS No. 4282-31-9, 6.02 €/g, Table S7 in ESI) if the DEF and water molecules are successfully removed from the cavities [98]. Also interesting are Zn_7-TDC_8 (VOLPET), with open tridimensionally connected pores, and CPM-202 (TAGTED), previously tested in CO_2 and CH_4 adsorption [99]. Zr-based DUT-69 (XICYIT) and DUT-67 (XICNOO) could store more than 50 g/L within their probed permanent porosity [100].

3,3',5,5'-Azobenzenetetracarboxylic acid (H_4AzBTC, CAS No. 365549-33-3, 22.29 €/g, Table S6 in ESI), the most expensive linker considered herein, yields seven MOFs overpassing 50 g/L of stored hydrogen coordinating Cu, Cd, and Zn. Material JUC-62 (OFOCUI, see Figure 9) with Cu is one of the listed MOFs in Table 1 that fulfil both gravimetric and volumetric hydrogen uptake [64]. The stability to moisture could be higher for Fe-based MOFs Fe_6-$AzTBC_3$ (IZENUY) and PCN-250' (TOWPEC) and in Al_6-$AzBTC_3$ (JALCAD). The hydrogen uptake of structure PCN-250' was experimentally determined to be up to 53 g/L, considering the measured density of the crystals [101]. Cr-based MIL-88D (YEDKUO) is the structure with the highest calculated volumetric uptake among the four reported structures from 4,4'-biphenyldicarboxylic acid (H_2bPDC, CAS No. 787-70-2, 0.29 €/g, Table S11 in ESI), which may also exhibit high stability to moisture. Structure UIO-67 (WIZMAV02) is a Zr-based MOF isorreticular to UIO-66 but containing expanded pores resulting in a higher surface area and pore volume. Despite the presence of Zr as metal, poor stability after ambient exposure was detected [101], probably because the used linker is larger than that for UIO-66 [89].

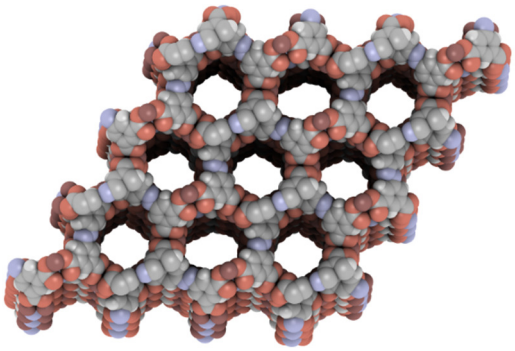

Figure 9. Material JUC-62 or Cu_4-$AzBTC_2$ (CSD code OFOCUI). Created with iRASPA [91].

N-donor linkers like azolates and pyridines are soft Lewis bases and tend to form strong metal-organic bonds with also soft Lewis acids like low-valence transition metal cations (like Co^{2+}, Ni^{2+}, Cu^{2+} and Zn^{2+}) [89]. The most used N-donor linker is 4,4'-Bipyridine (4,4'bPy, CAS No. 553-26-4, 0.21 €/g), which is

usually mixed with other linkers, but there are some single-linker examples (Table S5 in ESI). Cu clusters are used in structures Cu-4,4'bPy$_2$ (UXUPIN, UFUQIV, CUPHUS, and UXUNUX), where nitrogen atoms from the linker occupy the four positions in the square-plane of each Cu-octahedron, coordinating solvent molecules in the axial positions. These structures could potentially show OMS if they are stable after removing those solvent molecules. Up to 12 structures are deposited starting from 5-(4-pyridyl)tetrazol (PTz, CAS No. 14389-12-9, 19.26 €/g, see Table S9) as linker, where Cu-PTz (FUQJUX, see Figure 10) is the one with the highest potential hydrogen storage density up to 51 g/L.

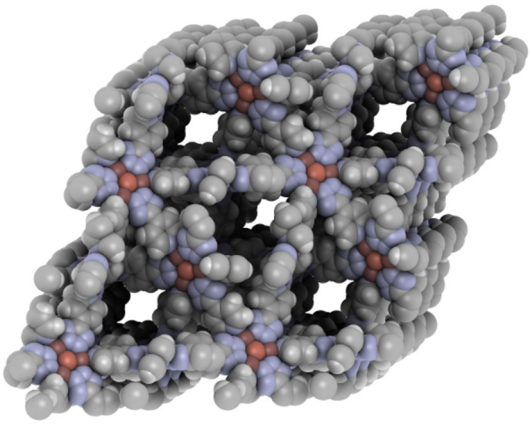

Figure 10. Structure Cu-PTz (CSD code FUQJUX). Created with iRASPA [91].

2-Methylimidazol (HMeIm, CAS No. 693-98-1, 0.04 €/g, Table S14 in ESI) is the azolate derivative with more deposited structures in this database to generally obtain ZIF compounds (Zeolitic Imidazolate Frameworks) coordinating Me^{2+} cations. The most known ZIF representative, commercially available, is the Zn-based material ZIF-8, one of the first examples of MOF with ultra-high thermal and chemical stabilities [102]. The Cd$_2$-MeIm (GUPCAW, see Figure 11), with a zeolitic MER topology instead of the SOD topology in ZIF-8 [103], shows the highest potential for volumetric hydrogen storage (ca. 50 g/L). Imidazole (Im, CAS No. 288-32-4, 0.02 €/g) is the next most frequently used azole, mainly coordinating tetrahedral Zn^{2+} cations in GIS-framework-type structures ZIF-6, ZIF-3, and ZIF-2. Structure Zn-Im$_2$ (HIFVOI) was not assigned to any zeolite structure but is similar to ZIF-6.

The linker Pyridine-3,5-dicarboxylic acid (H$_2$3,5PyDC, CAS No. 499-81-0, 0.29 €/g, Table S12 in ESI) or dinicotinic acid is simultaneously N- and O-donor linker and the stability of the resulting frameworks to acidic or basic media might be lower than that for a purely N- or O-donor linker [89]. However, the stability to ambient moisture could be enhanced since the structure holds one Me-linker strong bond (with either N- or O-donor), depending on the used metal. The structure Zn-PyDC (BUKMUQ, see Figure 12) could potentially store up to 60 g/L of H_2 if the structure is stable after removing the coordinated DMF molecules from Zn tetrahedra. Material Cu$_3$-PyDC$_2$ (EMUBOF) shows Cu-OMS, but its cavities are occupied by tetrakis(acetonitrile)-copper complexes, probably reducing the actual hydrogen uptake. Material JLU-Liu15 (EXAXAE) shows a similar structure to material HKUST-1, and was used for CO_2 selective adsorption for its capture and sequestration [104]. Another pyridine derivative, pyridine-4-carboxamide (P4CA, CAS No. 1453-82-3, 0.07 €/g, Table S13 in ESI) or isonicotinic acid, yields structures with OMS Cu$_2$-P4CA (QIWQES), Cd-P4CA (ROCZAM and UMABIV), and Ni$_9$-P4CA$_{10}$ (FEWTUY) with higher estimated uptake than 50 g/L.

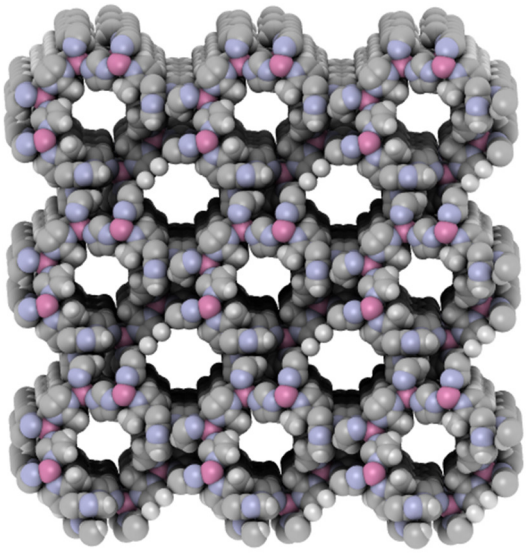

Figure 11. Structure Cd-$MeIm_2$ (CSD code GUPCAW). Created with iRASPA [91].

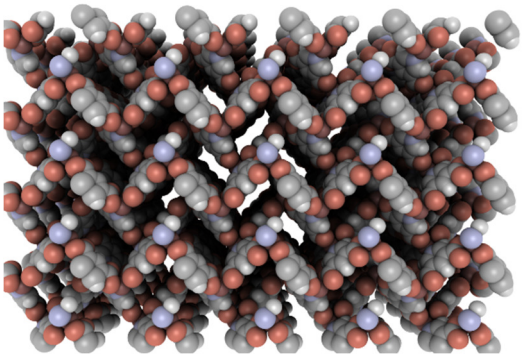

Figure 12. Structure Zn-PyDC (CSD code BUKMUQ). Created with iRASPA [91].

Besides pure linker MOFs, it is possible to find structures made out of more than one linker to coordinate single or mixed metal cations with remarkable volumetric hydrogen storage uptakes. Mixing linkers is a cheaper alternative than developing new linkers for constructing new MOF frameworks, opening new opportunities for structural versatility. Indeed, mixed-linker materials UMCM-1, -2, and 3, MOF-205, and -210 exhibit some of the highest reported porous properties [48]. Herein, 224 MOFs are selected from the combination of two linkers cheaper than 3,3',5,5'-Azobenzenetetracarboxylic acid and up to two metals. Structures with a third organic molecule are not selected, then those using extraframework ionic species like charge-balancing ions, structure-directing agents, or templates are not considered. Table 3 shows 19 interesting combinations of O-donor linkers, where the highest minimum uptake of 53.6 g/L was calculated for the combination of 1,4-benzenedicarboxylic acid and (2S)-2-amino-3-hydroxypropanic acid or serine (Ser, CAS No. 302-84-1, 0.12 €/g) with Zn, corresponding to the structure Zn_4-BDC-Ser_2 (RAPYOY, see Figure 13).

Structure Zn_4-BDC_3-Fa_2 (KOZNIY) out of 1,4-benzenedicarboxylic and formic acids (HFa, CAS No. 64-18-6, 0.02 €/g) also with Zn could store 50.4 g/L of hydrogen with the possibly cheapest combination of linkers and metals. Formic acid can be considered a linker in this structure since it can coordinate two different metal cations with each oxygen atom and become a Me-O-C-O-Me bridge. However, two or even more DEF molecules are coordinated to the octahedral Zn atoms, and their removal may cause a collapse of the structure. Similarly, using 4,4'-biphenyldicarboxylate as a second linker to coordinate Zn_4O clusters drives the formation of structure Zn_4-BDC_2-bPDC (FECZAQ), where DMF and water

molecules occupy the unsaturated sites by the linkers in the metallic nodes, potentially creating OMS after their removal. Thiophene-2,5-dicarboxylic and 4,4',4''-nitrilotribenzoic (H_3NOTB, CAS No. 118996-38-6, 19.09 €/g) acids coordinate Zn_4O clusters and could also exhibit OMS in the material NENU-521 (ZACHET). In structure Cd_6-BTC_4-BDC (EWECOY), terephthalic and trimesic acids coordinate helicoidal chains of Cd atoms reaching almost 50 g/L. Finally, coordinating octa-core aluminium-oxide clusters might show higher stability using a combination of the linker 1,3,5-tris(4-Carboxyphenyl)benzene with formic acid in structure Al_2-BTB-Fa (RIXPIZ).

Table 3. MOFs with mixed linkers from O-donor linkers.

Linker 1	Linker 2	Al	Cd	Cr Zn	Fe	Ni	Zn	Zr
1,4-benzenedicarboxylate								
	Formate						50.4	
	4,4'-biphenyldicarboxylate						50.1	
1,3,5-benzenetricarboxylate								
	1,4-Benzenedicarboxylate		50.9					
	Butane-1,4-diol					41.5		
Thiophene-2,5-dicarboxylate								
	Thiophene-2-carboxylate							47.9
	4,4',4''-nitrilotribenzoate						51.0	
4,4'-biphenyldicarboxylate								
	(2R)-2-hydroxy-2-phenylacetate						44.9	
	1,3,5-tris(4-Carboxyphenyl)benzene				52.7			
2-Nitrobenzene-1,4-dicarboxylate								
	1,4-Benzenedicarboxylate						49.6	
2-aminobenzene-1,4-dicarboxylate								
	1,3,5-tris(4-Carboxyphenyl)benzene						47.9	
2,6-naphtalenedicarboxylate								
	(2R)-2-hydroxy-2-phenylacetate						49.9	
2-hydroxybenzene-1,4-dicarboxylate								
	1,3,5-tris(4-Carboxyphenyl)benzene						48.4	
1,3,5-tris(4-Carboxyphenyl)benzene								
	Ethane-1,2-diolate	49.1						
	Formate	49.5						
	pyridine-4-carboxamide			50.7				

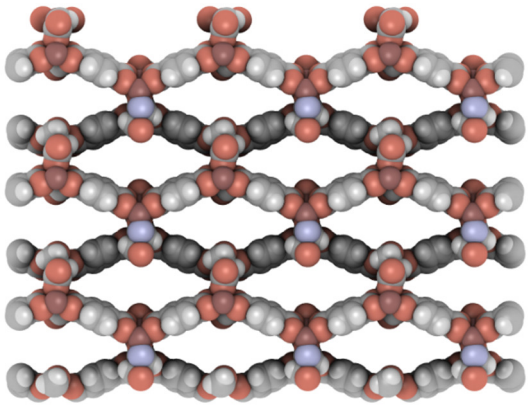

Figure 13. Structure Zn_4-BDC-Ser_2 (CSD code RAPYOY). Created with iRASPA [91].

Table 4 shows materials combining purely N-donor linkers with divalent Zn can Cu metals, then potentially reaching materials with high stability to water exposure and basic media. The best combination is imidazole and 2-Methylimidazole, which is able to store 48.4 g/L when they link Zn cations in the structure ZIF-60 (GITSUY) with MER topology. Higher uptakes are predicted when N-donor and O-donor moieties are mixed, i.e. carboxylated-based and azolates linkers with 34 possible combinations with higher predicted hydrogen uptake than 40 g/L.

Table 4. Mixed linkers MOFs from N-donor linkers.

Linker 1	Linker 2	Cu	Zn
Imidazole			
	2-Methylimidazole		48.3
	6-methyl-1H-benzimidazole		40.7
2-ethylimidazole			
	5-Methyltetrazole		42.9
Benzimidazole			
	2-Nitroimidazoleate		40.6
2-methyl-1H-benzo[d]imidazole			
	5-Methyltetrazole		42.1
1,2-bis(4-pyridyl)ethane			
	2,2'-Bipyridyl	40.4	
2-nitroimidazoleate			
	6-nitro-1H-benzimidazole		41.0
	6-methyl-1H-benzimidazole		40.2
	6-bromo-1H-benzimidazole		41.8
	Imidazole		48.0

The mixture of N-and O-donor functionalities has an unpredictable effect on materials' stability, and it should be tested for each material. Benzene-1,3-dicarboxylate and 3,5-dimethyl-1,2,4-triazole (3,5dMeTz, CAS No. 7343-34-2, 1.00 €/g) make structure Cu_9-IA_5-3,5dMeTz$_6$ (RUFZOJ) with 50.4 g/L of hydrogen uptake. To mix 1,3,5-benzenetricarboxylic acid and Benzotriazole (BTrz, CAS No. 95-14-7, 0.12 €/g) yields structures Zn_9-BTC_6-$BTrz_3$ (ZARLOV) and Zn_3-BTC_2-BTrz (NESVEO) with a minimum uptake of 52.7 g/L. 4,4'-ethene-1,2-diyldibenzoic acid (H_2EDB, CAS No. 100-31-2, 0.60 €/g) and 1,2,4-triazole (1,2,4TrAz, CAS No. 288-88-0, 0.04 €/g) generate the structure Zn_2-EDB-1,2,4TrAz$_2$ (CUQRUD) with the potential to store 50.9 g/L of hydrogen. Combination of 1,2,3-triazole (1,2,3TrAz, CAS No. 288-36-8, 0.68 €/g) with Thiophene-2,5-dicarboxylic acid and Zn generates the material TMOF (OMOVET), where all the coordination positions in the Zn octahedra are occupied by the second N atom from triazole creating reach N-Zn environments in a 3-fold interpenetrated framework [105].

Table 6 shows 32 combinations of carboxylates acids and bipyridines. 2,2'-bipyridyl (2,2'bPy, 366-18-7, 0.08 €/g) yields promising structures like that after mixing with 1,3,5-Benzenetricarboxylic acid to coordinate Zn atoms. In this structure, Mo-oxide clusters partially occupy the MOF cavities and reduce the available pore volume. The same happens with the combination of 2,2-bipyridyl with oxalic acid (H_2OA, CAS No. 144-62-7, 0.18 €/g), yielding the material NaCr-OA_3 (ZUQVAI), which creates a network where oxalate molecules link Cr and Na atoms and tris(Bipyridyl)-chromium clusters partially occupy the MOF cavities. 4,4'-bipyridine (4,4'bPy, 553-26-4, 0.21 €/g) is a more promising linker because it maximises the distance between nitrogen atoms in the linker, increasing the possibilities for creating a porous coordination polymer. Its combination with 5-aminobenzene-1,3-dicarboxylic acid (H_2NIA, CAS No. 99-31-0, 0.06 €/g) and Cu generates the structure Cu_4-NIA_4-4,4'bPy (IVEKEA) with open tridimensional porosity and potential OMS. In combination with biphenyl-4,4'-dicarboxylic acid and Cu, the tridimensional porous interwoven structure Cu_2-$bPDC_2$-4,4'bPy (EDOMAM) is obtained. The combination with 3,4-Pyridinedicarboxylic acid ($H_2$3,4PyDC, CAS No. 490-11-9, 0.30 €/g) and Cd creates the material JUC-67 (HOWQAM), whose permanent porosity can allocate 12 methanol molecules per unit cell [106]. Finally, the combination with 2,5-Dihydroxybenzene-1,4-dicarboxylic acid and Zn (Zn-DOTP-4,4bPy, SUPLOF) is potentially able to store 50.2 g/L of hydrogen.

There are 27 combinations of carboxylated and other pyridin- or pyrazin- derivatives to yield mixed linkers MOFs with potentially high hydrogen storage density shown in Table 7, like structure Zn_3Cr_3-BDC_3-$P4CA_6$ (XODPUD) from Benzene-1,4-dicarboxylic acid and isonicotinic acid. If 1,3,5-Benzenetricarboxylic acid is used as carboxylated linker, structure Zn_3Cr_3-BTC_2-$P4CA_6$ (SETSIV) is obtained with an even higher storage density. The synthesised material Zn_2-PyEty-OBZ_2 (DIDDOK, see Figure 14) from 4,4'-Oxydibenzoic acid (H_2OBZ_2, CAS No. 554-95-0, 0.12 €/g) and 1,2-bis(4-

pyridyl)ethylene (PyEty, CAS No. 13362-78-2, 6.27 €/g) shows a promising highly porous network where the three-dimensional framework contains large cavities about 13·11 Å² [107] for which 55.7 g/L of stored hydrogen density is estimated. Structure Cu_4-5OIA_4-Pyz (NIMQAD) out of 5-Hydroxybenzene-1,3-dicarboxylic acid ($H_2$5OIA, CAS No. 618-83-7, 0.19 €/g) and Pyrazine (Pyz, CAS No. 290-37-9, 0.58 €/g) linking Cu-paddle wheel clusters could store 51.2 g/L of hydrogen. 2,6-Naphtalenedicarboxylic acid and 4-(4-pyridyl)benzoic acid (HPBA, 4385-76-6, 12.28 €/g) and Ni creates the structure MCF-19-IIIb or Ni_6-NDC_3-PBA_6 (KARLUM), able to store ca. 42 g/L of hydrogen at 77 K and 50 bar [108]. Structure Zn_2-tBuIA-PyEt (NUMPAO) from 5-tert-butylbenzene-1,3-dicarboxylic acid (H_2tBuIA, CAS No. 2359-09-3, 1.37 €/g) and 1,2-bis(4-pyridyl)ethane (PyEt, 4916-57-8, 6.17 €/g) could store 53 g/L of hydrogen. Finally, 1,3,5-tris(4-Carboxyphenyl)benzene and pyridine-4-carboxamide coordinate Zn and Cr atoms to generate the structure Cr_3Zn_3-BTB_2-$P4CA_6$ (SETSUH) with an uptake of 50.6 g/L.

Table 5. MOFs from mixed carboxylates and azolates linkers.

		Cd			Fe			Zn	
Linker 1	Linker 2	Ca	Cd	Cu	Cu	Mg	Mn	Cu	Zn
1,2,4,5-Benzenetetracarboxylate									
	2H-tetrazol-5-amine								40.7
1,3,5-Benzenetricarboxylate									
	1,2,4-triazolyl								42.5
	2-imidazoleidone		46.1						
	1,4-bis(imidazole-1-ylmethyl)benzene		53.7						
1,4-Benzenedicarboxylate									
	1,2,4-triazolyl					44.4			44.5
	2-imidazoleidone	44.0	42.5						
	1H-1,2,4-triazol-5-amine		47.0						
	1,2,3-triazole								50.7
	5-Methyltetrazole		45.1						
	5-(4-pyridyl)tetrazol		44.1						
benzene-1,3-dicarboxylate									
	3,5-dimethyl-1,2,4-triazolate			50.4					47.5
2,5-Dihydroxybenzene-1,4-dicarboxylate									
	1,2,4-triazolyl				48.0				
2,6-Naphtalenedicarboxylate									
	1,3,4-Oxadiazole								47.2
	5-Methyltetrazole								40.4
2-aminobenzene-1,4-dicarboxylate									
	1,2,4-triazolyl								43.3
3,3',5,5'-Azobenzenetetracarboxylate									
	4,4'-sulfonyldibenzoate						47.3		
4,4'-biphenyldicarboxylate									
	1H-1,2,4-triazol-5-amine		50.0						
	4-(3,5-Dimethyl-1H-pyrazol-4-yl)pyridine								46.4
4,4'-ethene-1,2-diyldibenzoate									
	1,2,4-triazolyl		48.6						50.8
4,4'-methanediylbis(3-hydroxynaphthalene-2-carboxylate)									
	3,5-diamino-1,2,4-triazol-1-yl								48.7
	1,4-bis(imidazole-1-ylmethyl)benzene		42.0						
5-Hydroxybenzene-1,3-dicarboxylate									
	2-imidazoleidone		46.5						
Benzene-1,2,4-tricarboxylate									
	1,2,4-triazolyl								47.2
Formate									
	1,2,3-triazole							48.9	
Thiophene-2,5-dicarboxylate									
	1,2,4-triazolyl								44.1
	1,2,3-triazole								50.4

Table 6. MOFs from mixed carboxylated and bipyridine linkers.

Linker 1	Linker 2	Mo Zn	Cd	Na Cr	Cu	Fe	Mn	Ni	Zn
2,2'-dipyridylamine									
	Benzene-1,2-dicarboxylate		41.3						
2,2'-bipyridyl									
	1,3,5-Benzenetricarboxylate	55.1							
	Oxalate			52.7					
	1,3,5-tris(4-Carboxyphenyl)benzene								48.2
4,4'-bipyridine									
	Malate							48.7	
	Ethylenediaminetetraacetate				43.6				
	Formate					42.1		43.9	
	Pyridine-4-carboxamide		40.2						
	5-aminobenzene-1,3-dicarboxylate				51.4				
	1,3,5-Benzenetricarboxylate							43.0	43.5
	4,4'-Oxydibenzoate						41.4		
	5-Hydroxybenzene-1,3-dicarboxylate				49.3				46.2
	5-sulfobenzene-1,3-dicarboxylate								46.8
	3,3',3''-(2,4,6-trioxo-1,3,5-triazinane-1,3,5-triyl)tripropanoate				47.9				
	4,4'-biphenyldicarboxylate				50.0				40.3
	1,2,2-trimethylcyclopentane-1,3-dicarboxylate				41.5				
	3,4-Pyridinedicarboxylate		51.9						
	Imidazole-4,5-dicarboxylate		41.4						
	4,4'-ethene-1,2-diyldibenzoate								41.3
	2-aminobenzene-1,4-dicarboxylate		47.7						
	2,6-Naphtalenedicarboxylate								42.6
	2,5-Dihydroxybenzene-1,4-dicarboxylate								50.2
	4,4'-carbonyldibenzoate				46.2				
	Benzene-1,2,3-tricarboxylate				41.6				
	1,3,5-tris(4-Carboxyphenyl)benzene		43.8		49.2				49.0
	9-oxofluorene-2,7-dicarboxylate								45.6
2,2'-Bipyridine-5,5'-dicarboxylate									
	Formate								52.5

Finally, some MOFs are made by combining carboxylated-based linkers with different N-bonding moieties than those in the previous tables, like purines, diazabicyclo or hexamethyltetraamino compounds. Table 8 shows the most interesting combinations, like 1,4-diazabicyclo[2.2.2]octane (1,4dAzbCy, CAS No. 280-57-9, 0.12 €/kg) and benzene-1,3-dicarboxylate coordinating Zn-oxide clusters in a paddle-wheel configuration, resulting in the structure Zn_4-IA_4-1,4dAzbCy (FORXAM) which could store 51.9 g/L of hydrogen. If 1,4-Benzenedicarboxylic acid is used to coordinate Zn, the material Zn_2-BDC_2-1,4dAzbCy (WARFAY01) could store 52.5 g/L. With a mixture of Cu and Zn, the material CuZn-BDC_2-1,4dAzbCy (WARFIG) could store 52.5 g/L. Finally, Fe_2-BDC_2-1,4dAzbCy (XIVVEF) and Ni-BDC_2-1,4dAzbCy (EZOFUV) could store 51.6 and 50.3 g/L, respectively. Terephthalic acid can also be substituted by 4,4'-biphenyldicarboxylic acid yielding the structure Zn_2-$bPDC_2$-1,4dAzbCy (FEFDEB), with 50.6 g/L. Also promising, but more expensive, are the combinations of diazabicyclo[2.2.2]octane with 4,4'-carbonyldibenzoic acid ($H_2$4,4'COdB, CAS No. 964-68-1, 3.47 €/g) in Zn_2-4,4'$COdB_2$-1,4dAzbCy (HOHMIB), and with 4,4'-(1,1,1,3,3,3-Hexafluoropropane-2,2-diyl)dibenzoic acid (H_2F_6PdB, CAS No. 1171-47-7, 5.65 €/g) in Zn_2-F_6PdB_2-1,4dAzbCy (WIHWAN).

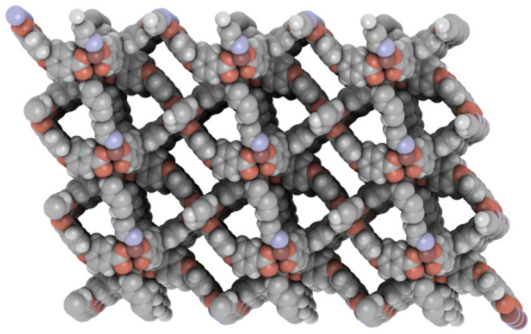

Figure 14. Structure Zn_2-$(OBZ_2)_2$(PyEty) (CSD code DIDDOK). Created with iRASPA [91].

Table 7. MOFs from mixed carboxylates linkers and other pyridin- or pyrazin- derivatives.

Linker 1	Linker 2	Cd	Cu	Fe	Ni	Zn Cr	Zn
Benzene-1,3-dicarboxylate							
	Pyridine-4-carboxamide				40.2		
	1,3-bis(4-Pyridyl)propane		41.2				
1,4-benzenedicarboxylate							
	Pyridine-3-carboxylate			45.1	45.1		
	Pyridine-4-carbonitrile			45.0			
	Pyridine-4-carboxamide					51.0	
	1,3-bis(4-Pyridyl)propane	42.1					48.5
	Pyrazine				44.1		
	4-(4-pyridyl)benzoate						47.4
1,3,5-benzenetricarboxylate							
	Pyridine-4-carboxamide					52.3	
	Pyrazine				44.9		
4,4'-oxydibenzoate							
	1,2-bis(4-pyridyl)ethylene						55.7
5-Hydroxybenzene-1,3-dicarboxylate							
	Pyrazine		51.2				
5-sulfobenzene-1,3-dicarboxylate							
	Pyrazine		55.0				
3,4-pyridinedicarboxylate							
	Hexamethylenetetraamino	45.0					49.7
4,4'-biphenyldicarboxylate							
	1,2-bis(4-pyridyl)ethane			47.9			
Furan-2,5-dicarboxylate							
	1,3-bis(4-Pyridyl)propane						40.8
2,6-naphtalenedicarboxylate							
	1,3-bis(4-Pyridyl)propane	46.9					
	1,2-bis(4-pyridyl)ethylene						48.8
	4-(4-pyridyl)benzoate				50.5		
5-tert-butylbenzene-1,3-dicarboxylate							
	1,2-bis(4-pyridyl)ethane						52.6
2-hydroxybenzene-1,4-dicarboxylate							
	Pyrazine	46.2					
2,6-dimethylpyridine-3,5-dicarboxylate							
	Pyridine-4-carboxamide				48.1		
Benzene-1,2,3,4,5-pentacarboxylate							
	1,2-bis(4-pyridyl)ethane	45.0					
1,3,5-tris(4-Carboxyphenyl)benzene							
	Pyridine-4-carboxamide					50.6	

Table 8. MOFs from mixed carboxylates linkers and other N-binding linkers.

Linker 1	Linker 2	Cd	Cu Zn	Cu	Fe	Ni	Zn
7H-purin-6-amine							
	pyridine-4-carboxamide	48.8					40.1
1,4-diazabicyclo[2.2.2]octane							
	benzene-1,3-dicarboxylate						51.9
	1,4-Benzenedicarboxylate		52.5	52.5	51.8	50.3	49.7
	4,4'-biphenyldicarboxylate						50.6
	5-methylbenzene-1,3-dicarboxylate						49.2
	2,6-Naphtalenedicarboxylate					46.0	
	2,5-Dichloro-1,4-benzenedicarboxylate						47.1
	4,4'-carbonyldibenzoate						51.1
	4,4'-(1,1,1,3,3,3-Hexafluoropropane-2,2-diyl)dibenzoate						50.8
	2-hydroxybenzene-1,4-dicarboxylate						48.5
hexamethylenetetraamino							
	Thiophene-2,5-dicarboxylate	43.0					
	3,4-Pyridinedicarboxylate	45.0					

Conclusions

The requirements from DOE for volumetric hydrogen storage can be achieved at cryogenic temperature in many different MOF materials synthesized so far. Herein, we elaborated a selection of almost 4,000 structures from the CoRE MOF database obtained from industrially relevant metals and estimated hydrogen uptake from 40 g/L at 77 K and 100 bar, predicted from their calculated porous properties. Also, listing the organic composition of materials, we elaborated a MOF database with crystallographic, structural, chemical, and porous properties, where the available laboratory-use cost of the organic linkers, if they are commercially available, is also collected. This database allows comparing MOFs' composition and performance in hydrogen storage, helping to evaluate the most feasible candidates for industrial production. Herein, we showed that the highest volumetric storage density can be achieved by using expensive linkers, but it is still possible to obtain several candidates with high volumetric uptake from the cheapest ones, like terephthalic or trimesic acids, and also combining up to two metals and three linkers to provide better performance and improved stability than the material MOF-5, the most studied material for this aim.

Up to 666 MOF structures from individual linkers and metals can show successful operation for hydrogen storage using cheaper linkers than 3,3',5,5'-azobenzenetetracarboxylic acid, the linker of the commercially available material PCN-250(Fe). The most frequent metal-organic combination is 1,4-benzenedicarboxylic acid and Zn, for which MOF-5 (CSD Code MIBQAR) is the most known example, but other structures like Zn_3-BDC_4 (CSD code UFENAW) show potential storage density up to 62 g/L. Structures UIO-66, MIL-88B, -53, -101, and -47 show lower hydrogen uptake but could be more stable to moisture. Trimesic or 1,3,5-Benzenetricarboxylic acid is the second most-used linker to yield MOFs coordinating Cu nodes like in HKUST-1, but the combination with Zn (material BIT-103) could store a higher amount of hydrogen. Structures Fe_6-BTC_3, Mn_3-BTC_2, and Cr_3-BTC_2, with lower uptake, might be more stable. Structure CAU-3-NDC out of 2,6-Naphthalenedicarboxylic acid and Al could store almost 50 g/L of hydrogen in a stable structure, as well as structures DUT-67 and -69 from Zr and Thiophene-2,5-dicarboxylic acid. N-donor linkers like azolate derivatives linking divalent metals are stable materials, like ZIF-8, but their estimated uptakes are generally lower than those from carboxylated linkers. Mixing N- and O-donor groups in the linker improves the porosity and can enhance stability.

The structure Zn-PyDC from Pyridine-3,5-dicarboxylic acid (BUKMUQ) could potentially store up to 60 g/L of H_2.

In addition to single-linker MOFs, 224 promising MOF structures are constructed from combinations of up to two linkers and two metals. Structures Zn_4-BDC-Ser_2 (RAPYOY) out of 1,4-benzenedicarboxylic acid, (2S)-2-amino-3-hydroxypropanic acid, and Zn; and structure Zn_4-BDC_3-Fa_2 (KOZNIY) from of 1,4-benzenedicarboxylic and formic acids, are examples of structures with higher hydrogen uptake than 50 g/L from the combination of the cheapest O-donor linkers. The combination of N-donor linkers yields structures with lower hydrogen uptake, but this is improved by mixing N- and O-donor linkers, like carboxylates and imidazolates. That is the case of the structure Cu_9-IA_5-3,5dMeTz_6 (RUFZOJ) after mixing Benzene-1,3-dicarboxylate and 3,5-dimethyl-1,2,4-triazole for potentially storing more than 50 g/L of hydrogen, or 1,3,5-benzenetricarboxylic acid and Benzotriazole with even higher storage density. The combination of 1,2,3-triazole with Thiophene-2,5-dicarboxylic acid and Zn could also store more than 50 g/L. Also interesting are combinations of 4,4'-bipyridyl with carboxylic acids like 5-aminobenzene-1,3-dicarboxylate, biphenyl-4,4'-dicarboxylate, 3,4-Pyridinedicarboxylate, and 2,5-Dihydroxybenzene-1,4-dicarboxylate resulting in structures with higher storage capacity than 50 g/L. Different derivatives from pyridine or from pyrazine can be also used as N-donor linkers, like Pyridine-4-carboxamide, 1,2-bis(4-pyridyl)ethane, 1,2-bis(4-pyridyl)ethylene, Pyrazine, and 4-(4-pyridyl)benzoate.

In addition to the selection of materials in this database, the identification of versatile cheap components opens the possibility of creating derivatives from existing MOFs or even new structures from these affordable building blocks. In addition to hydrogen uptake and porosity, crystalline and chemical properties are collected in this database, allowing the selection of structures for applications like catalysis or gas separation. Finally, a user interface allows the creation of customized MOF selections detailing the CSD reference, name of the structure, porous and crystalline properties, gravimetric and volumetric total uptakes, and metallic and organic composition. Structure search is possible from the properties of the organic linkers, like name (or partial name), molecular mass, price, or presence of specific functional groups, being also possible to specify the number of metallic or organic components in the materials. This information can be useful *per se* as a tool to find promising structures for their industrial production for hydrogen storage or other applications. It can also be used as starting information for new ML or IA approaches for selecting materials based on their composition.

List or abbreviations

Abbreviation	**Name of the substance**
Ser	(2S)-2-amino-3-hydroxypropanoic acid or Serine
1,2,3TrAz	1,2,3-triazole
1,2,4TrAz	1,2,4-triazole
PyEt	1,2-bis(4-pyridyl)ethane
PyEty	1,2-bis(4-pyridyl)ethylene
H3BTC	1,3,5-Benzenetricarboxylic or trimesic acid
H3BTB	1,3,5-tris(4-Carboxyphenyl)benzene
H2BDC	1,4-benzenedicarboxylic or terephthalic acid
1,4bMeImB	1,4-bis(imidazole-1-yl-methyl)benzene
1,4dAzbCy	1,4-diazabicyclo[2.2.2]octane

2,2'bPy	2,2'-Bipyridine
H2DOTP	2,5-Dihydroxybenzene-1,4-dicarboxylic acid
DOBQ	2,5-dioxy-1,4-benzoquinone
H2NDC	2,6-Naphthalenedicarboxylic acid
HMeIm	2-Methylimidazol
H4AzBTC	3,3’,5,5'-Azobenzenetetracarboxylic acid
3,5dMeTz	3,5-dimethyl-1,2,4-triazole
HPBA	4-(4-pyridyl)benzoic acid
H2F6PdB	4,4’-(1,1,1,3,3,3-Hexafluoropropane-2,2-diyl)dibenzoic acid
H3NOTB	4,4’,4''-nitrilotribenzoic acid
H2bPDC	4,4'-biphenyldicarboxylic acid
4,4'bPy	4,4'-Bipyridine
H24,4´COdB	4,4'-carbonyldibenzoic acid
H2EDB	4,4'-ethene-1,2-diyldibenzoic acid
3PTz	5-(4-pyridyl)tetrazol
H25OIA	5-Hydroxybenzene-1,3-dicarboxylic acid
H2tBuIA	5-tert-butylbenzene-1,3-dicarboxylic acid
H2IA	Benzene-1,3-dicarboxylic or isophthalic acid
BTrz	Benzotriazole
Hfa	Formic acid
Im	Imidazole
H2OA	Oxalic acid
Pyz	Pyrazine
3,5H2PyDC	pyridine-3,5-dicarboxylic acid
3,4H2PyDC	pyridine-3,5-dicarboxylic acid
P4CA	pyridine-4-carboxamide or isonicotinic acid
H2TDC	Thiophene-2,5-dicarboxylic acid

References

1. Richtie, H.; Roser, M. *Energy mix*. 2020 [2022 18/03/2022]; Available from: https://ourworldindata.org/energy.
2. Rissman, J.; Bataille, C.; Masanet, E.; Aden, N.; Morrow, W.R.; Zhou, N.; Elliott, N.; Dell, R.; Heeren, N.; Huckestein, B.; Cresko, J.; Miller, S.A.; Roy, J.; Fennell, P.; Cremmins, B.; Blank, T.K.; Hone, D.; Williams, E.D.; du Can, S.D.; Sisson, B.; Williams, M.; Katzenberger, J.; Burtraw, D.; Sethi, G.; Ping, H.; Danielson, D.; Lu, H.Y.; Lorber, T.; Dinkel, J.; Helseth, J. Technologies and policies to decarbonize global industry: Review and assessment of mitigation drivers through 2070. *Appl Energ* **2020**, *266*, 114848. DOI: 10.1016/j.apenergy.2020.114848.
3. Poullikkas, A. Sustainable options for electric vehicle technologies. *Renew Sust Energ Rev* **2015**, *41*, 1277-1287. DOI: 10.1016/j.rser.2014.09.016.
4. Cipriani, G.; Di Dio, V.; Genduso, F.; La Cascia, D.; Liga, R.; Miceli, R.; Galluzzo, G.R. Perspective on hydrogen energy carrier and its automotive applications. *Int J Hydrogen Energ* **2014**, *39*, 8482-8494. DOI: 10.1016/j.ijhydene.2014.03.174.
5. Dutta, S. A review on production, storage of hydrogen and its utilization as an energy resource. *J Ind Eng Chem* **2014**, *20*, 1148-1156. DOI: 10.1016/j.jiec.2013.07.037.

6. Kélouwani, S.; Agbossou, K.; Chahine, R. Model for energy conversion in renewable energy system with hydrogen storage. *J of Power Sources* **2005**, *140*, 392-399. DOI: 10.1016/j.jpowsour.2004.08.019.

7. Eberle, U.; Felderhoff, M.; Schuth, F. Chemical and physical solutions for hydrogen storage. **2009**, *48*, 6608-30. DOI: 10.1002/anie.200806293.

8. Andersson, J.; Gronkvist, S. Large-scale storage of hydrogen. *Int J Hydrogen Energ* **2019**, *44*, 11901-11919. DOI: 10.1016/j.ijhydene.2019.03.063.

9. Pham, T.; Forrest, K.A.; Banerjee, R.; Orcajo, G.; Eckert, J.; Space, B. Understanding the H2 Sorption Trends in the M-MOF-74 Series (M = Mg, Ni, Co, Zn). *J Phys Chem C* **2014**, *119*, 1078-1090. DOI: 10.1021/jp510253m.

10. Zhou, L.; Zhou, Y.P.; Sun, Y. Enhanced storage of hydrogen at the temperature of liquid nitrogen. *Int J Hydrogen Energ* **2004**, *29*, 319-322. DOI: 10.1016/S0360-3199(03)00155-1.

11. Sun, Y.; Wang, L.; Amer, W.A.; Yu, H.; Ji, J.; Huang, L.; Shan, J.; Tong, R. Hydrogen Storage in Metal-Organic Frameworks. *J Inorg Organomet P* **2012**, *23*, 270-285. DOI: 10.1007/s10904-012-9779-4.

12. Schlichtenmayer, M.; Hirscher, M. Nanosponges for hydrogen storage. *J Mater Chem* **2012**, *22*, 10134-10143. DOI: 10.1039/c2jm15890f.

13. Myers, A.L. Thermodynamics of adsorption in porous materials. *Aiche J* **2002**, *48*, 145-160. DOI: DOI 10.1002/aic.690480115.

14. Poirier, E.; Dailly, A. On the nature of the adsorbed hydrogen phase in microporous metal-organic frameworks at supercritical temperatures. *Langmuir* **2009**, *25*, 12169-76. DOI: 10.1021/la901680p.

15. Valenti, G., *Hydrogen liquefaction and liquid hydrogen storage*, in *Compendium of Hydrogen Energy*. 2016, Woodhead Publishing. p. 27-51.

16. Ball, M.; Weeda, M. The hydrogen economy - Vision or reality? *Int J Hydrogen Energ* **2015**, *40*, 7903-7919. DOI: 10.1016/j.ijhydene.2015.04.032.

17. Ramirez-Vidal, P.; Sdanghi, G.; Celzard, A.; Fierro, V. High hydrogen release by cryo-adsorption and compression on porous materials. *Int J Hydrogen Energ* **2022**, *47*, 8892-8915. DOI: 10.1016/j.ijhydene.2021.12.235.

18. Dalebrook, A.F.; Gan, W.; Grasemann, M.; Moret, S.; Laurenczy, G. Hydrogen storage: beyond conventional methods. *Chem Commun* **2013**, *49*, 8735-51. DOI: 10.1039/c3cc43836h.

19. Niaz, S.; Manzoor, T.; Pandith, A.H. Hydrogen storage: Materials, methods and perspectives. *Renew Sust Energ Rev* **2015**, *50*, 457-469. DOI: 10.1016/j.rser.2015.05.011.

20. Kalidindi, S.B.; Fischer, R.A. Covalent organic frameworks and their metal nanoparticle composites: Prospects for hydrogen storage. *Phys Status Solidi B* **2013**, *250*, 1119-1127. DOI: 10.1002/pssb.201248477.

21. Batten, S.R.; Champness, N.R.; Chen, X.M.; Garcia-Martinez, J.; Kitagawa, S.; Ohrstrom, L.; O'Keeffe, M.; Suh, M.P.; Reedijk, J. Terminology of metal-organic frameworks and coordination polymers (IUPAC Recommendations 2013). *Pure Appl Chem* **2013**, *85*, 1715-1724. DOI: 10.1351/Pac-Rec-12-11-20.

22. Tranchemontagne, D.J.; Mendoza-Cortes, J.L.; O'Keeffe, M.; Yaghi, O.M. Secondary building units, nets and bonding in the chemistry of metal-organic frameworks. *Chem Soc Rev* **2009**, *38*, 1257-83. DOI: 10.1039/b817735j.

23. O'Keeffe, M.; Yaghi, O.M. Deconstructing the crystal structures of metal–organic frameworks and related materials into their underlying nets. **2011**, *112*, 675-702.

24. Moghadam, P.Z.; Li, A.; Wiggin, S.B.; Tao, A.; Maloney, A.G.P.; Wood, P.A.; Ward, S.C.; Fairen-Jimenez, D. Development of a Cambridge Structural Database Subset: A Collection of Metal-Organic Frameworks for Past, Present, and Future. *Chem Mater* **2017**, *29*, 2618-2625. DOI: 10.1021/acs.chemmater.7b00441.

25. Rosi, N.L.; Eckert, J.; Eddaoudi, M.; Vodak, D.T.; Kim, J.; O'Keeffe, M.; Yaghi, O.M. Hydrogen storage in microporous metal-organic frameworks. **2003**, *300*, 1127-9. DOI: 10.1126/science.1083440.

26. Kaye, S.S.; Dailly, A.; Yaghi, O.M.; Long, J.R. Impact of preparation and handling on the hydrogen storage properties of Zn4O(1,4-benzenedicarboxylate)3 (MOF-5). *J Am Chem Soc* **2007**, *129*, 14176-7. DOI: 10.1021/ja076877g.

27. Farha, O.K.; Yazaydin, A.O.; Eryazici, I.; Malliakas, C.D.; Hauser, B.G.; Kanatzidis, M.G.; Nguyen, S.T.; Snurr, R.Q.; Hupp, J.T. De novo synthesis of a metal-organic framework material featuring ultrahigh surface area and gas storage capacities. *Nat Chem* **2010**, *2*, 944-8. DOI: 10.1038/nchem.834.

28. Ahmed, A.; Seth, S.; Purewal, J.; Wong-Foy, A.G.; Veenstra, M.; Matzger, A.J.; Siegel, D.J. Exceptional hydrogen storage achieved by screening nearly half a million metal-organic frameworks. *Nat Commun* **2019**, *10*, 1568. DOI: 10.1038/s41467-019-09365-w.

29. Broom, D.P.; Webb, C.J.; Fanourgakis, G.S.; Froudakis, G.E.; Trikalitis, P.N.; Hirscher, M. Concepts for improving hydrogen storage in nanoporous materials. *Int J Hydrogen Energ* **2019**, *44*, 7768-7779. DOI: 10.1016/j.ijhydene.2019.01.224.

30. Balderas-Xicohténcatl, R.; Schlichtenmayer, M.; Hirscher, M. Volumetric Hydrogen Storage Capacity in Metal–Organic Frameworks. *Energy Technol-GER* **2018**, *6*, 578-582. DOI: 10.1002/ente.201700636.

31. Furukawa, H.; Cordova, K.E.; O'Keeffe, M.; Yaghi, O.M. The chemistry and applications of metal-organic frameworks. **2013**, *341*, 1230444. DOI: 10.1126/science.1230444.

32. Gomez, D.A.; Toda, J.; Sastre, G. Screening of hypothetical metal-organic frameworks for H2 storage. *Phys Chem Chem Phys* **2014**, *16*, 19001-10. DOI: 10.1039/c4cp01848f.

33. Ding, L.F.; Yazaydin, A.O. Hydrogen and methane storage in ultrahigh surface area Metal-Organic Frameworks. *Micropor Mesopor Mat* **2013**, *182*, 185-190. DOI: 10.1016/j.micromeso.2013.08.048.

34. Ahmed, A.; Liu, Y.Y.; Purewal, J.; Tran, L.D.; Wong-Foy, A.G.; Veenstra, M.; Matzger, A.J.; Siegel, D.J. Balancing gravimetric and volumetric hydrogen density in MOFs. *Energ Environ Sci* **2017**, *10*, 2459-2471. DOI: 10.1039/c7ee02477k.

35. Goldsmith, J.; Wong-Foy, A.G.; Cafarella, M.J.; Siegel, D.J. Theoretical Limits of Hydrogen Storage in Metal-Organic Frameworks: Opportunities and Trade-Offs. *Chem Mater* **2013**, *25*, 3373-3382. DOI: 10.1021/cm401978e.

36. Chen, Z.; Kirlikovali, K.O.; Li, P.; Farha, O.K. Reticular Chemistry for Highly Porous Metal-Organic Frameworks: The Chemistry and Applications. *Acc Chem Res* **2022**, *55*, 579-591. DOI: 10.1021/acs.accounts.1c00707.

37. Ryu, U.; Jee, S.; Rao, P.C.; Shin, J.; Ko, C.; Yoon, M.; Park, K.S.; Choi, K.M. Recent advances in process engineering and upcoming applications of metal-organic frameworks. *Coord Chem Rev* **2021**, *426*, 213544. DOI: 10.1016/j.ccr.2020.213544.

38. Sud, D.; Kaur, G. A comprehensive review on synthetic approaches for metal-organic frameworks: From traditional solvothermal to greener protocols. *Polyhedron* **2021**, *193*, 114897. DOI: 10.1016/j.poly.2020.114897.

39. Chen, Z.; Wasson, M.C.; Drout, R.J.; Robison, L.; Idrees, K.B.; Knapp, J.G.; Son, F.A.; Zhang, X.; Hierse, W.; Kuhn, C.; Marx, S.; Hernandez, B.; Farha, O.K. The state of the field: from inception to commercialization of metal-organic frameworks. *Faraday Discuss* **2021**, *225*, 9-69. DOI: 10.1039/d0fd00103a.

40. Shet, S.P.; Priya, S.S.; Sudhakar, K.; Tahir, M. A review on current trends in potential use of metal-organic framework for hydrogen storage. *Int J Hydrogen Energ* **2021**, *46*, 11782-11803. DOI: 10.1016/j.ijhydene.2021.01.020.

41. Sule, R.; Mishra, A.K.; Nkambule, T.T. Recent advancement in consolidation of MOFs as absorbents for hydrogen storage. *Int J Energ Res* **2021**, *45*, 12481-12499. DOI: 10.1002/er.6608.

42. DeSantis, D.; Mason, J.A.; James, B.D.; Houchins, C.; Long, J.R.; Veenstra, M. Techno-economic Analysis of Metal-Organic Frameworks for Hydrogen and Natural Gas Storage. *Energ Fuel* **2017**, *31*, 2024-2032. DOI: 10.1021/acs.energyfuels.6b02510.

43. Severino, M.I.; Gkaniatsou, E.; Nouar, F.; Pinto, M.L.; Serre, C. MOFs industrialization: a complete assessment of production costs. *Faraday Discuss* **2021**, *231*, 326-341. DOI: 10.1039/d1fd00018g.

44. Peng, P.; Anastasopoulou, A.; Brooks, K.; Furukawa, H.; Bowden, M.E.; Long, J.R.; Autrey, T.; Breunig, H. Cost and potential of metal-organic frameworks for hydrogen back-up power supply. *Nat Energy* **2022**, *7*, 448-458. DOI: 10.1038/s41560-022-01013-w.

45. Chung, Y.G.; Haldoupis, E.; Bucior, B.J.; Haranczyk, M.; Lee, S.; Zhang, H.D.; Vogiatzis, K.D.; Milisavljevic, M.; Ling, S.L.; Camp, J.S.; Slater, B.; Siepmann, J.I.; Sholl, D.S.; Snurr, R.Q. Advances, Updates, and Analytics for the Computation-Ready, Experimental Metal-Organic Framework Database: CoRE MOF 2019. *J Chem Eng Data* **2019**, *64*, 5985-5998. DOI: 10.1021/acs.jced.9b00835.

46. Zhao, D.; Yuan, D.Q.; Zhou, H.C. The current status of hydrogen storage in metal-organic frameworks. *Energ Environ Sci* **2008**, *1*, 222-235. DOI: 10.1039/b808322n.

47. Sculley, J.; Yuan, D.Q.; Zhou, H.C. The current status of hydrogen storage in metal-organic frameworks-updated. *Energ Environ Sci* **2011**, *4*, 2721-2735. DOI: 10.1039/c1ee01240a.

48. Suh, M.P.; Park, H.J.; Prasad, T.K.; Lim, D.W. Hydrogen storage in metal-organic frameworks. *Chem Rev* **2012**, *112*, 782-835. DOI: 10.1021/cr200274s.

49. Furukawa, H.; Miller, M.A.; Yaghi, O.M. Independent verification of the saturation hydrogen uptake in MOF-177 and establishment of a benchmark for hydrogen adsorption in metal-organic frameworks. *J Mater Chem* **2007**, *17*, 3197-3204. DOI: 10.1039/b703608f.

50. Furukawa, H.; Ko, N.; Go, Y.B.; Aratani, N.; Choi, S.B.; Choi, E.; Yazaydin, A.O.; Snurr, R.Q.; O'Keeffe, M.; Kim, J.; Yaghi, O.M. Ultrahigh porosity in metal-organic frameworks. *Science* **2010**, *329*, 424-8. DOI: 10.1126/science.1192160.

51. Hirscher, M. Hydrogen storage by cryoadsorption in ultrahigh-porosity metal-organic frameworks. *Angew Chem Int Ed* **2011**, *50*, 581-2. DOI: 10.1002/anie.201006913.

52. Wong-Foy, A.G.; Matzger, A.J.; Yaghi, O.M. Exceptional H2 saturation uptake in microporous metal-organic frameworks. *J Am Chem Soc* **2006**, *128*, 3494-5. DOI: 10.1021/ja058213h.

53. Dinca, M.; Dailly, A.; Liu, Y.; Brown, C.M.; Neumann, D.A.; Long, J.R. Hydrogen storage in a microporous metal-organic framework with exposed Mn2+ coordination sites. *J Am Chem Soc* **2006**, *128*, 16876-83. DOI: 10.1021/ja0656853.

54. Park, H.J.; Lim, D.W.; Yang, W.S.; Oh, T.R.; Suh, M.P. A highly porous metal-organic framework: structural transformations of a guest-free MOF depending on activation method and temperature. *Chem Eur J* **2011**, *17*, 7251-60. DOI: 10.1002/chem.201003376.

55. Lee, Y.G.; Moon, H.R.; Cheon, Y.E.; Suh, M.P. A comparison of the H2 sorption capacities of isostructural metal–organic frameworks with and without accessible metal sites:[{Zn2 (abtc)(dmf) 2} 3] and [{Cu2 (abtc)(dmf) 2} 3] versus [{Cu2 (abtc)} 3]. *Angew Chem* **2008**, *120*, 7855-7859. DOI: 10.1002/ange.200801488.

56. Wong-Foy, A.G.; Lebel, O.; Matzger, A.J. Porous crystal derived from a tricarboxylate linker with two distinct binding motifs. *J Am Chem Soc* **2007**, *129*, 15740-1. DOI: 10.1021/ja0753952.

57. Lin, X.; Telepeni, I.; Blake, A.J.; Dailly, A.; Brown, C.M.; Simmons, J.M.; Zoppi, M.; Walker, G.S.; Thomas, K.M.; Mays, T.J.; Hubberstey, P.; Champness, N.R.; Schroder, M. High capacity hydrogen adsorption in Cu(II) tetracarboxylate framework materials: the role of pore size, ligand functionalization, and exposed metal sites. *J Am Chem Soc* **2009**, *131*, 2159-71. DOI: 10.1021/ja806624j.

58. Yang, S.; Lin, X.; Dailly, A.; Blake, A.J.; Hubberstey, P.; Champness, N.R.; Schröder, M. Enhancement of H2 adsorption in coordination framework materials by use of ligand curvature. *Chemistry–Eur J* **2009**, *15*, 4829-4835.

59. Yan, Y.; Lin, X.; Yang, S.; Blake, A.J.; Dailly, A.; Champness, N.R.; Hubberstey, P.; Schroder, M. Exceptionally high H2 storage by a metal-organic polyhedral framework. *Chem Commun* **2009**, 1025-7. DOI: 10.1039/b900013e.

60. Yan, Y.; Blake, A.J.; Lewis, W.; Barnett, S.A.; Dailly, A.; Champness, N.R.; Schroder, M. Modifying cage structures in metal-organic polyhedral frameworks for H2 storage. *Chem Eur J* **2011**, *17*, 11162-70. DOI: 10.1002/chem.201101341.

61. Wang, X.S.; Ma, S.Q.; Rauch, K.; Simmons, J.M.; Yuan, D.Q.; Wang, X.P.; Yildirim, T.; Cole, W.C.; Lopez, J.J.; de Meijere, A.; Zhou, H.C. Metal-organic frameworks based on double-bond-coupled di-isophthalate linkers with high hydrogen and methane uptakes. *Chem Mater* **2008**, *20*, 3145-3152. DOI: 10.1021/cm800403d.

62. Zhao, D.; Yuan, D.; Yakovenko, A.; Zhou, H.C. A NbO-type metal-organic framework derived from a polyyne-coupled di-isophthalate linker formed in situ. *Chem Commun* **2010**, *46*, 4196-8. DOI: 10.1039/c002767g.

63. Yuan, D.; Zhao, D.; Sun, D.; Zhou, H.C. An isoreticular series of metal-organic frameworks with dendritic hexacarboxylate ligands and exceptionally high gas-uptake capacity. *Angew Chem Int Ed Engl* **2010**, *49*, 5357-61. DOI: 10.1002/anie.201001009.

64. Xue, M.; Zhu, G.S.; Li, Y.X.; Zhao, X.J.; Jin, Z.; Kang, E.; Qiu, S.L. Structure, hydrogen storage, and luminescence properties of three 3D metal-organic frameworks with NbO and PtS topologies. *Cryst Growth Des* **2008**, *8*, 2478-2483. DOI: 10.1021/cg8001114.

65. Rowsell, J.L.; Yaghi, O.M. Effects of functionalization, catenation, and variation of the metal oxide and organic linking units on the low-pressure hydrogen adsorption properties of metal-organic frameworks. *J Am Chem Soc* **2006**, *128*, 1304-15. DOI: 10.1021/ja056639q.

66. Bryant, S. *Download scripts for the CSD Python API from the CSD GitHub repository*. 2022 [2022 2022-04-22]; Available from: https://www.ccdc.cam.ac.uk/Community/blog/download-csd-python-api-scripts-github/#how-to-use-csd-github-repo.

67. Bucior, B.J.; Rosen, A.S.; Haranczyk, M.; Yao, Z.P.; Ziebel, M.E.; Farha, O.K.; Hupp, J.T.; Siepmann, J.I.; Aspuru-Guzik, A.; Snurr, R.Q. Identification Schemes for Metal-Organic Frameworks To Enable Rapid Search and Cheminformatics Analysis. *Cryst Growth Des* **2019**, *19*, 6682-6697. DOI: 10.1021/acs.cgd.9b01050.

68. Warr, W.A. Representation of chemical structures. *Wires Comput Mol Sci* **2011**, *1*, 557-579. DOI: 10.1002/wcms.36.

69. O'Boyle, N.M.; Banck, M.; James, C.A.; Morley, C.; Vandermeersch, T.; Hutchison, G.R. Open Babel: An open chemical toolbox. *J Cheminform* **2011**, *3*, 33. DOI: 10.1186/1758-2946-3-33.

70. Heller, S.R.; McNaught, A.; Pletnev, I.; Stein, S.; Tchekhovskoi, D. InChI, the IUPAC International Chemical Identifier. *J Cheminform* **2015**, *7*, 23. DOI: 10.1186/s13321-015-0068-4.

71. Chong, S.; Lee, S.; Kim, B.; Kim, J. Applications of machine learning in metal-organic frameworks. *Coordin Chem Rev* **2020**, *423*, 213487. DOI: ARTN 213487

10.1016/j.ccr.2020.213487.

72. Jablonka, K.M.; Ongari, D.; Moosavi, S.M.; Smit, B. Big-Data Science in Porous Materials: Materials Genomics and Machine Learning. **2020**, *120*, 8066-8129. DOI: 10.1021/acs.chemrev.0c00004.

73. Rosen, A.S.; Iyer, S.M.; Ray, D.; Yao, Z.P.; Aspuru-Guzik, A.; Gagliardi, L.; Notestein, J.M.; Snurr, R.Q. Machine learning the quantum-chemical properties of metal-organic frameworks for accelerated materials discovery. *Matter-Us* **2021**, *4*, 1578-1597. DOI: 10.1016/j.matt.2021.02.015.

74. Wang, Z.H.; Zhou, Y.G.; Zhou, T.; Sundmacher, K. Identification of optimal metal-organic frameworks by machine learning: Structure decomposition, feature integration, and predictive modeling. *Comput Chem Eng* **2022**, *160*, 107739. DOI: 10.1016/j.compchemeng.2022.107739

10.1016/j.compchemeng.2022.107739.

75. Petuya, R.; Durdy, S.; Antypov, D.; Gaultois, M.W.; Berry, N.G.; Darling, G.R.; Katsoulidis, A.P.; Dyer, M.S.; Rosseinsky, M.J. Machine-Learning Prediction of Metal-Organic Framework Guest Accessibility from Linker and Metal Chemistry. *Angew Chem Int Ed Engl* **2022**, *61*, e202114573. DOI: 10.1002/anie.202114573.

76. Luo, Y.; Bag, S.; Zaremba, O.; Cierpka, A.; Andreo, J.; Wuttke, S.; Friederich, P.; Tsotsalas, M. MOF Synthesis Prediction Enabled by Automatic Data Mining and Machine Learning. *Angew Chem Int Ed Engl* **2022**, *61*, e202200242. DOI: 10.1002/anie.202200242.

77. Villajos, J.A.; Zimathies, A.; Prinz, C. A fast procedure for the estimation of the hydrogen storage capacity by cryoadsorption of metal-organic framework materials from their available porous properties. **2020**.

78. Cambridge, U.o. *OPSIN: Open Parser for Systematic IUPAC nomenclature*. 2009 2019-07-13; Available from: https://opsin.ch.cam.ac.uk/.

79. Information, N.C.f.B. *PubChem*. [2020; Available from: https://pubchem.ncbi.nlm.nih.gov/.

80. Villajos, J.A.; Zimathies, A.; Prinz, C. A fast procedure for the estimation of the hydrogen storage capacity by cryoadsorption of metal-organic framework materials from their available porous properties. *Int J Hydrogen Energ* **2021**, *46*, 29323-29331. DOI: 10.1016/j.ijhydene.2020.10.265.

81. Düren, T.; Millange, F.; Férey, G.; Walton, K.S.; Snurr, R.Q. Calculating Geometric Surface Areas as a Characterization Tool for Metal−Organic Frameworks. *J Phys Chem C* **2007**, *111*, 15350-15356. DOI: 10.1021/jp074723h.

82. Broom, D.P.; Hirscher, M. Irreproducibility in hydrogen storage material research. *Energ Environ Sci* **2016**, *9*, 3368-3380. DOI: 10.1039/c6ee01435f.

83. Hurst, K.E.; Gennett, T.; Adams, J.; Allendorf, M.D.; Balderas-Xicohtencatl, R.; Bielewski, M.; Edwards, B.; Espinal, L.; Fultz, B.; Hirscher, M.; Hudson, M.S.L.; Hulvey, Z.; Latroche, M.; Liu, D.J.; Kapelewski, M.; Napolitano, E.; Perry, Z.T.; Purewal, J.; Stavila, V.; Veenstra, M.; White, J.L.; Yuan, Y.; Zhou, H.C.; Zlotea, C.; Parilla, P. An International Laboratory Comparison Study

of Volumetric and Gravimetric Hydrogen Adsorption Measurements. *Chemphyschem* **2019**, *20*, 1997-2009. DOI: 10.1002/cphc.201900166.

84. García-Holley, P.; Schweitzer, B.; Islamoglu, T.; Liu, Y.; Lin, L.; Rodriguez, S.; Weston, M.H.; Hupp, J.T.; Gómez-Gualdrón, D.A.; Yildirim, T.; Farha, O.K. Benchmark Study of Hydrogen Storage in Metal–Organic Frameworks under Temperature and Pressure Swing Conditions. *ACS Energy Lett* **2018**, *3*, 748-754. DOI: 10.1021/acsenergylett.8b00154.

85. Chun, H.; Seo, J. Discrimination of small gas molecules through adsorption: reverse selectivity for hydrogen in a flexible metal-organic framework. *Inorg Chem* **2009**, *48*, 9980-2. DOI: 10.1021/ic901456k.

86. Reich, M.; Vasconcelos, P.M. Geological and Economic Significance of Supergene Metal Deposits. *Elements* **2015**, *11*, 305-310. DOI: 10.2113/gselements.11.5.305.

87. Zhou, W.; Wu, H.; Yildirim, T. Enhanced H2 adsorption in isostructural metal-organic frameworks with open metal sites: strong dependence of the binding strength on metal ions. *J Am Chem Soc* **2008**, *130*, 15268-9. DOI: 10.1021/ja807023q.

88. Dalapati, R.; Sakthivel, B.; Dhakshinamoorthy, A.; Buragohain, A.; Bhunia, A.; Janiak, C.; Biswas, S. A highly stable dimethyl-functionalized Ce(IV)-based UiO-66 metal-organic framework material for gas sorption and redox catalysis. *Crystengcomm* **2016**, *18*, 7855-7864. DOI: 10.1039/c6ce01704e.

89. Yuan, S.; Feng, L.; Wang, K.; Pang, J.; Bosch, M.; Lollar, C.; Sun, Y.; Qin, J.; Yang, X.; Zhang, P.; Wang, Q.; Zou, L.; Zhang, Y.; Zhang, L.; Fang, Y.; Li, J.; Zhou, H.C. Stable Metal-Organic Frameworks: Design, Synthesis, and Applications. *Adv Mater* **2018**, *30*, e1704303. DOI: 10.1002/adma.201704303.

90. Winarta, J.; Shan, B.; Mcintyre, S.M.; Ye, L.; Wang, C.; Liu, J.; Mu, B. A decade of UiO-66 research: a historic review of dynamic structure, synthesis mechanisms, and characterization techniques of an archetypal metal–organic framework. *Cryst Growth Des* **2019**, *20*, 1347-1362. DOI: 10.1021/acs.cgd.9b00955.

91. Dubbeldam, D.; Calero, S.; Vlugt, T.J.H. iRASPA: GPU-accelerated visualization software for materials scientists. *Mol Simulat* **2018**, *44*, 653-676. DOI: 10.1080/08927022.2018.1426855.

92. Chavan, S.M.; Zavorotynska, O.; Lamberti, C.; Bordiga, S. H2 interaction with divalent cations in isostructural MOFs: a key study for variable temperature infrared spectroscopy. *Dalton Trans* **2013**, *42*, 12586-95. DOI: 10.1039/c3dt51312b.

93. Vitillo, J.G.; Regli, L.; Chavan, S.; Ricchiardi, G.; Spoto, G.; Dietzel, P.D.; Bordiga, S.; Zecchina, A. Role of exposed metal sites in hydrogen storage in MOFs. *J Am Chem Soc* **2008**, *130*, 8386-96. DOI: 10.1021/ja8007159.

94. Liu, Y.; Kabbour, H.; Brown, C.M.; Neumann, D.A.; Ahn, C.C. Increasing the density of adsorbed hydrogen with coordinatively unsaturated metal centers in metal-organic frameworks. *Langmuir* **2008**, *24*, 4772-7. DOI: 10.1021/la703864a.

95. Dietzel, P.D.; Georgiev, P.A.; Eckert, J.; Blom, R.; Strassle, T.; Unruh, T. Interaction of hydrogen with accessible metal sites in the metal-organic frameworks M(2)(dhtp) (CPO-27-M; M = Ni, Co, Mg). *Chem Commun* **2010**, *46*, 4962-4. DOI: 10.1039/c0cc00091d.

96. Zuluaga, S.; Fuentes-Fernandez, E.M.A.; Tan, K.; Xu, F.; Li, J.; Chabal, Y.J.; Thonhauser, T. Understanding and controlling water stability of MOF-74. *J Mater Chem A* **2016**, *4*, 5176-5183. DOI: 10.1039/c5ta10416e.

97. Klimakow, M.; Klobes, P.; Thunemann, A.F.; Rademann, K.; Emmerling, F. Mechanochemical Synthesis of Metal-Organic Frameworks: A Fast and Facile Approach toward Quantitative

Yields and High Specific Surface Areas. *Chem Mater* **2010**, *22*, 5216-5221. DOI: 10.1021/cm1012119.

98. Eddaoudi, M.; Kim, J.; Vodak, D.; Sudik, A.; Wachter, J.; O'Keeffe, M.; Yaghi, O.M. Geometric requirements and examples of important structures in the assembly of square building blocks. *Proc Natl Acad Sci U S A* **2002**, *99*, 4900-4. DOI: 10.1073/pnas.082051899.

99. Zhai, Q.G.; Bu, X.H.; Zhao, X.; Mao, C.Y.; Bu, F.; Chen, X.T.; Feng, P.Y. Advancing Magnesium-Organic Porous Materials through New Magnesium Cluster Chemistry. *Cryst Growth Des* **2016**, *16*, 1261-1267. DOI: 10.1021/acs.cgd.5b01297.

100. Bon, V.; Senkovska, I.; Baburin, I.A.; Kaskel, S. Zr- and Hf-Based Metal-Organic Frameworks: Tracking Down the Polymorphism. *Cryst Growth Des* **2013**, *13*, 1231-1237. DOI: 10.1021/cg301691d.

101. Villajos, J.A. Experimental volumetric hydrogen uptake determination at 77 K of commercially available metal-organic framework materials. *C* **2022**, *8*, 5. DOI: 10.3390/c8010005.

102. Park, K.S.; Ni, Z.; Cote, A.P.; Choi, J.Y.; Huang, R.; Uribe-Romo, F.J.; Chae, H.K.; O'Keeffe, M.; Yaghi, O.M. Exceptional chemical and thermal stability of zeolitic imidazolate frameworks. *Proc Natl Acad Sci U S A* **2006**, *103*, 10186-10191. DOI: 10.1073/pnas.0602439103.

103. Tian, Y.Q.; Yao, S.Y.; Gu, D.; Cui, K.H.; Guo, D.W.; Zhang, G.; Chen, Z.X.; Zhao, D.Y. Cadmium imidazolate frameworks with polymorphism, high thermal stability, and a large surface area. *Chem.–Eur. J* **2010**, *16*, 1137-41. DOI: 10.1002/chem.200902729.

104. Surble, S.; Serre, C.; Mellot-Draznieks, C.; Millange, F.; Ferey, G. A new isoreticular class of metal-organic-frameworks with the MIL-88 topology. *Chem Commun* **2006**, 284-6. DOI: 10.1039/b512169h.

105. Qin, J.S.; Du, D.Y.; Li, M.; Lian, X.Z.; Dong, L.Z.; Bosch, M.; Su, Z.M.; Zhang, Q.; Li, S.L.; Lan, Y.Q.; Yuan, S.; Zhou, H.C. Derivation and Decoration of Nets with Trigonal-Prismatic Nodes: A Unique Route to Reticular Synthesis of Metal-Organic Frameworks. *J Am Chem Soc* **2016**, *138*, 5299-307. DOI: 10.1021/jacs.6b01093.

106. Xue, M.; Zhu, G.S.; Ding, H.; Wu, L.; Zhao, X.J.; Jin, Z.; Qiu, S.L. Six Three-Dimensional Metal-Organic Frameworks with (3,4)-, (4,5)-, and (3,4,5)-Connected Nets Based on Mixed Ligands: Synthesis, Structures, and Adsorption Properties. *Cryst Growth Des* **2009**, *9*, 1481-1488. DOI: 10.1021/cg8009546.

107. Kondo, M.; Irie, Y.; Miyazawa, M.; Kawaguchi, H.; Yasue, S.; Maeda, K.; Uchida, F. Synthesis and structural determination of new multidimensional coordination polymers with 4,4 '-oxybis(benzoate) building ligands: Construction of coordination polymers with heteroorganic bridges. *J Organomet Chem* **2007**, *692*, 136-141. DOI: 10.1016/j.jorganchem.2006.07.048.

108. Zhang, Y.B.; Zhou, H.L.; Lin, R.B.; Zhang, C.; Lin, J.B.; Zhang, J.P.; Chen, X.M. Geometry analysis and systematic synthesis of highly porous isoreticular frameworks with a unique topology. *Nat Commun* **2012**, *3*, 642. DOI: 10.1038/ncomms1654.